HHS Public Access

Author manuscript

Oncogene. Author manuscript; available in PMC 2013 July 17.

Published in final edited form as:

Oncogene. 2013 January 17; 32(3): 327–340. doi:10.1038/onc.2012.52.

Role of MMP-2 in the Regulation of IL-6/Stat3 Survival Signaling via Interaction With α5β1 Integrin in glioma

Divya Kesanakurti[1], **Chandramu Chetty**[1], **Dzung H. Dinh**[2], **Meena Gujrati**[3], and **Jasti S. Rao**[1,2,*]

[1]Department of Cancer Biology and Pharmacology, University of Illinois College of Medicine at Peoria, One Illini Drive, Peoria, IL 61605, U.S.A.

[2]Department of Neurosurgery, University of Illinois College of Medicine at Peoria, One Illini Drive, Peoria, IL 61605, U.S.A.

[3]Department of Pathology, University of Illinois College of Medicine at Peoria, One Illini Drive, Peoria, IL 61605, U.S.A.

Abstract

MMP-2 plays pivotal role in the degradation of extracellular matrix, and thereby enhances the invasive, proliferative and metastatic potential in cancer. Knockdown of MMP-2 using MMP-2 siRNA (pM) in human glioma xenograft cell lines 4910 and 5310 decreased cell proliferation compared to mock- and pSV-(scrambled vector)treatments, as determined by BrDU incorporation, Ki-67 staining and clonogenic survival assay. Cytokine array and Western blotting using tumor conditioned media displayed modulated secretory levels of various cytokines including GM-CSF, IL-6, IL-8, IL-10, TNF-α, angiogenin, VEGF and PDGF-BB in MMP-2 knockdown cells. Further, cDNA PCR array indicated potential negative regulation of JAK/Stat3 pathway in pM-treated cells. Mechanistically, MMP-2 is involved in complex formation with α5 and β1 integrins and MMP-2 downregulation inhibited α5β1 integrin mediated Stat3 phosphorylation and nuclear translocation. EMSA and ChIP assays showed inhibited Stat3 DNA-binding activity and recruitment at CyclinD1 and c-Myc promoters in pM-treated cells. In individual experiments, IL-6 or siRNA-insensitive MMP-2 overexpression by pM-FL-A141G counteracted and restored the pM-inhibited Stat3 DNA-binding activity suggesting IL-6/Stat3 signaling suppression in pM-treated 4910 and 5310 cells. MMP-2/α5β1 binding is enhanced in rhMMP-2 treatments resulting in elevated Stat3 DNA-binding activity and recruitment on CyclinD1 and c-Myc promoters. Activation of α5β1 signaling by Fibronectin adhesion elevated pM-inhibited Stat3 phosphorylation whereas blocking α5β1 abrogated constitutive Stat3 activation. *In vivo* experiments with orthotropic tumor model revealed the decreased tumor size in pM-treatment compared to mock- or pSV-treatments. Immunoflorescence studies in tumor sections corroborated

[*]**Corresponding Author:** Jasti S. Rao, Ph.D., Department of Cancer Biology & Pharmacology, University of Illinois College of Medicine, One Illini Drive, Peoria, IL 61605, U.S.A.; phone: 309-671-3445; jsrao@uic.edu.

CONFLICT OF INTEREST

The authors declare no conflicts of interest exist with this manuscript.

our *in vitro* findings evidencing high expression and co-localization of MMP-2/α5β1, which is decreased upon pM-treatment along with significantly reduced IL-6, phospho-Stat3, CyclinD1, c-Myc, Ki-67 and PCNA expression levels. Our data indicates the possible role of MMP-2/α5β1 interaction in the regulation of α5β1-mediated IL-6/Stat3 signaling activation and signifies the therapeutic potential of blocking MMP-2/α5β1 interaction in glioma treatment.

Keywords

MMP-2; α5β1; glioma; IL-6; STAT3; CyclinD1; c-Myc

INTRODUCTION

High proliferative and invasive behavior of malignant tumors of the central nervous system is responsible for inefficacy of existing treatment procedures (1). Glioma malignancy is, in part, attributed to the action of a group of metallo-, cysteine and serine proteases, which degrade extracellular matrix (ECM) proteins (2, 3). Matrix metalloproteinase-2 (MMP-2) is a 72 kDa, Zn^{+2}-dependent secreted endopeptidase and its elevated expression is highly correlated with increased tumor progression implicating its multiple roles in tumor cell proliferation, migration, invasion, and angiogenesis (4). Enhanced glioma malignancy is also characterized by aberrant expression of integrins, which comprises 18 α and 8 β subunits that combine to form about 24 heterodimers, and their dynamic interactions with ECM molecules generate intracellular oncogenic signaling events (5). Several studies demonstrated the significance of MMP-2/αVβ3 integrin liaison in the regulation of tumor proliferation, invasion, and angiogenesis (6–9). Along with αVβ3, integrin α5β1 (Very Late Antigen 5, VLA5) is also implicated to enhance tumor progression by triggering various survival signaling pathways including PI3K-AKT, Bcl-2, and NF-κB (10–14). Recently accumulating evidences shows α5β1-mediated modulation of MMP-2 activity and suggests a direct interaction between MMP-2 and α5 integrin in melanoma and breast cancer cells (15–17). Migrating astrocytes show co-localization of MMP-2 with β1 integrin at the cell periphery, indicating its significance in pericellular proteolysis (18). However, knowledge on MMP-2/α5β1 interaction and its role in the regulation of α5β1-mediated signaling pathways in glioma is still lacking.

Tumor progression is orchestrated by an intricate set of cytokines which play key roles in attenuation of apoptosis and enhanced invasion and metastases of cancer tissue (8, 19). Interleukin-6 (IL-6) belongs to a family of cytokines participating in gp130 receptor signaling in the activation of JAK/Stat3 activation in several cancers including glioblastoma and high circulating IL-6 levels are associated with increased tumor malignancy (20–24). Upon stimulation, IL-6 binds to sIL-6R, which then induces gp130 dimerization and Janus kinases (JAKs) phosphorylation which facilitate recruitment, phosphorylation, and subsequent nuclear translocation of STAT (Signal Transducers and Activators of Transcription) proteins (25) Persistent Stat3 activation is a hallmark of several human cancers, and it acts as a critical transcriptional mediator of oncogenic signaling, enhancing cancer cell proliferation, migration, and angiogenesis via activation of its target genes, which encode anti-apoptotic and angiogenic factors (26–30). High Stat3 activity is

correlated with enhanced MMP-2 activity, which is itself a Stat3 target gene and blockade of Stat3 activity by dominant-negative-Stat3 or treatment with JAK-inhibitor significantly reduced MMP activity (31–33). Specific inhibition of the of Stat3 signaling cascade inhibited invasion and migration in glioma and tumor growth in lung cancer (22, 34, 35).

Our previous studies with MMP-2 knockdown in human lung cancer and glioma cell lines inhibited proliferation, invasion, and migration and led to apoptotic cell death (36) Based on the complexity of integrin signaling and our preliminary cytokine expression analysis of the culture supernatants (which revealed a significant suppression of several cytokines under MMP-2 depleted conditions), we sought to determine the possible modulation of β1 integrin-mediated IL-6/Stat3 activation and its implication in MMP-2.siRNA-induced cell death in human glioma xenograft cell lines. Taken together, the detailed analysis of constitutive Stat3 inhibition with MMP-2.siRNA and α5β1 blocking treatments confirmed the substantial interaction of MMP-2/α5β1 integrin by immunocomplex formation and further elucidates the mechanistic role of MMP-2/α5β1 in IL-6/Stat3 signaling activation in glioma.

RESULTS

MMP-2 knockdown inhibited human glioma xenograft cell proliferation

The significant inhibition in MMP-2 expression and activity in pM-treated 4910 and 5310 cells in comparison to mock- and pSV- treated cells at 48 h was confirmed by RT-PCR, Western blotting and gelatin zymography (Supplementary Figure S1A). BrDU proliferation assay at pre-determined time intervals indicated that the pM-transfected cells showed a time-dependent decrease in proliferation rate from 24 to 96 hours compared to mock and pSV-treated cells. A significant inhibition in proliferation up to 56.5% (72 hours) and 66.1% (96 hours) was documented in pM-treated 4910 cells. The 5310 cells displayed 56.2% and 65.4% decrease in BrDU incorporation at 72 and 96 hours of post-transfection, respectively (Figure 1A). Immunofluorescence showed decreased nuclear Ki-67 staining in pM-treated cells compared to mock- and pSV-treated controls (Figure 1B). Further, monolayer colony formation assay showed severe hindrance in the colony forming efficiency of pM-treated cells (Figure 1C). After 10 days, there was up to ≥70.8% and ≥71.2% inhibition in colony formation in pM-treated 4910 and 5310 cells respectively when compared to their control counterparts (Figure 1D).

MMP-2 downregulation decreased α5 and β1 integrin expression and MMP-2/α5β1 interaction

A possible interaction between MMP-2 and α5β1 has been implicated in the modulation of MMP-2 activity and subsequent tumor cell invasion has been reported previously in melanoma and breast cancer cells (15–17). Several reports suggested the positive regulation of survival signaling by α5β1 integrin and targeting by α5β1 antagonists decreased proliferation in tumor cells (37, 38). Based on the previous reports suggesting possible MMP-2/α5β1 integrin interaction and with the prominent proliferation inhibition upon MMP-2 downregulation in our studies we next checked the effect of MMP-2 knockdown on α5 and β1 integrin expression levels. Both α5 and β1 mRNA and protein expression levels

were remarkably reduced and densitometric analysis showed up to ~60% reduction in pM-treated 4910 and 5310 cells compared to control counterparts (Supplementary Fig. S1B, Figure 2A). Immunoprecipitation experiments showed immunocomplex formation of MMP-2/α5 and MMP-2/β1 by physical interaction in un-treated 4910 and 5310 cells whereas pM-treated cells show decreased interaction (Figure 2B). Eventually co-IP blots were re-probed with antibody used for immunoprecipitation to check the band specificity, input samples were subjected to Western blotting, and GAPDH levels were estimated to confirm equal loading. Confocal studies signified a strong co-localization of MMP-2 with α5β1 in mock- and pSV-treated 4910 and 5310 cells. On the other hand, pM-transfected cells showed noticeable inhibition in MMP-2 and α5β1 expression, which subsequently led to decreased MMP-2/α5β1 co-localization. Densitometric analysis showed significant reduction (up to ~67%) in MMP-2/α5β1 co-localization upon pM-treatment for 48 hours (Figure 2C). To further verify the MMP-2/α5β1 interaction, we overexpressed siRNA-insensitive Myc-tagged MMP-2 (pM-FL-A141G) in 4910 and 5310 cells. MMP-2 overexpression was confirmed by Western blotting analysis in comparison to mock or pEV controls (Supplementary Fig. S1C). Immunoprecipitation and probing with anti-MMP-2 and anti-Myc antibodies confirmed enhanced MMP-2/α5β1 binding in pM-FL-A141G treated cells compared to mock and pEV control counterparts (Supplementary Fig. S1C). siRNA-insensitive MMP-2 overexpression upon pM-FL-A141G treatment was confirmed by Western blotting (Supplementary Fig. S1D). The prominent decreases in MMP-2 and α5β1 expression levels and interaction in pM treatments and enhancement of MMP-2/α5β1 binding by pM-FL-A141G treatment suggests a role of MMP-2 binding in α5β1 integrin-mediated intracellular signaling. The high expression and co-localization of MMP-2 and α5β1 integrin was also evident in the human glioblastoma tissues implicating the significance of MMP-2/α5β1 binding in glioma malignancy where as normal brain tissues did not show noticeable expression and MMP-2/α5β1 co-localization (Supplementary Figure S2).

MMP-2 downregulation altered cytokine secretion pattern in glioma xenograft cells

The tumor microenvironment is characterized by enhanced cytokine levels, which in turn activates signaling pathways facilitating exacerbation of proliferation, differentiation, and invasion of the tumor cells (19). With the prominent reduction of proliferation in MMP-2 knockdown cells, we next sought to evaluate the secretory cytokine profile in the extracellular milieu. As described in Materials and Methods, conditioned media consisting of secretory cytokines and growth factors was collected from pSV- and pM-treated cells and subjected to cytokine array which indicated a prominent modulation in cytokine release pattern with an inhibition in several cytokines including GM-CSF, IL-6, IL-8, IL-10, TNF-α, Angiogenin, VEGF, and PDGF-BB in MMP-2-knockdown cells. Densitometric analysis of cytokine array showed significant ($p<0.01$) and moderate ($p<0.05$) differences among pSV and pM treatments. Upon pM-treatment a significant inhibition in GM-CSF, IL-6, IL-8, IL-10, VEGF, and PDGF-BB (at $p<0.01$) and a moderate decrease in TNF-α ($p<0.05$) was documented in both 4910 and 5310 cells (Figure 3A). Angiogenin showed a noticeable inhibition of up to ~71% in 4910 and a moderate loss up to ~48% in 5310 cells, respectively. This noticeable reduction in the secretion levels of GM-CSF, IL-6, IL-8, IL-10, TNF-α, Angiogenin, VEGF, PDGF BB was further confirmed by subjecting conditioned media to

Western blot analysis in both 4910 and 5310 cell lines (Figure 3B). The significant loss of cytokine secretion is in correlation with the reduction of cellular expression levels of cytokines IL-6, IL-8 and IL-10 in MMP-2 knockdown 4910 and 5310 cells (Figure 3C).

MMP-2 depletion altered JAK/STAT pathway gene expression

Interleukin-6 is one of the abundantly expressed cytokine in the tumor microenvironment, which binds to gp130 receptor and subsequently activates JAK/STAT survival signaling. Based on the striking downregulation of cellular and secreted IL-6 levels in pM-treated cells, we further checked the possible modulation Stat3 signaling pathway genes by performing JAK/STAT pathway PCR array and compared gene expression profiles in pSV- and pM- treated cells. The significant fold change deviation from threshold value were indicated which included the genes encoding JAK receptor proteins, other interacting proteins, and Stat3-target proteins. Among the various downregulated Stat3 signaling related genes, the essential receptor proteins such as EGFR (epidermal growth factor receptor); IL-6ST (gp130); IL2RG (Interleukin 2 receptor, gamma); IL1-RA (Interleukin 10 receptor, alpha); IL-4R (Interleukin 4 receptor); Tyk2 (Tyrosine kinase 2); JAK2 (Janus kinase 2) and Csf2rb (Colony stimulating factor 2 receptor, beta), showed decreased expression implying a modulation of expression of several receptor proteins in the pM treatment group of both cell lines (Table 1). The PCR array analysis also revealed a noticeable downregulation in Stat3 target genes encoding for c-Myc, Bcl-2L1, CyclinD1 and upregulation in Stat3 signaling suppressors including PIAS1, SOCS1, CDKI1A and PP2Aα confirming the potential negative regulation of Stat3 pathway in MMP-2 depleted cells.

MMP-2 depletion inhibited constitutive Stat3 activation in glioma xenograft cells

Western blotting showed considerable decrease in gp130, phospho-JAK1, JAK1, phospho-JAK2, JAK2 and phospho-Stat3 (Tyr-705 and Ser-727) expression levels with no noticeable change in total Stat3 in pM-treated 4910 and 5310 cells whereas constitutive Stat3 activation were documented in both mock- and pSV-treated controls (Figure 4A). Even though the inhibition in Stat3 phosphorylation was evident at 24 h we observed further decrease at 48 hours post pM-transfection indicating that this effect was time-dependent (data not shown). Fluorescence microscopy showed conspicuous reduction in phospho-Stat3 expression and subsequent nuclear translocation in MMP-2 knockdown cells. In contrast, mock- and pSV-treated cells show high expression of phospho-Stat3 distributed throughout cytoplasm, with prominent nuclear localization (Figure 4B). To further assess the effect of pM on Stat3 DNA-binding activity, EMSA was performed which revealed a high Stat3 activity in both mock- and pSV-treated 4910 and 5310 controls. Conversely, a prominent decrease in DNA-binding activity was evidenced in 48 h pM-transfected cells implying that the loss of MMP-2 leads to suppression of constitutive STAT3 activation (Figure 4C). Further, the recruitment of Stat3 was assessed by ChIP assay which showed a strong occupancy of Stat3 at CyclinD1 and c-Myc promoters in both mock- and pSV-treated 4910 and 5310 cells. In contrast, MMP-2 suppression using pM noticeably inhibited the Stat3 recruitment on to CyclinD1 and c-Myc promoters suggesting the downregulation of these proteins (Figure 4D). Western blotting showed a remarkable downregulation in Stat3 target proteins CyclinD1, c-Myc, Bcl-xL, Bcl2 and Survivin in pM-treated 4910 and 5310 cells in comparison to control counterparts (Figure 4E). Eventually, to rule out the off-target effects

of pM on negative regulation of α5β1-mediated IL-6/Stat3 activation and proliferation in 4910 and 5310 cell lines, parallel MMP-2 knockdown experiments were also performed using pM-1 (siRNA in pcDNA3.0 targeting the 1073–1094 position in MMP-2 cDNA), pM-2 (sc-29398) and siRNA-specific scrambled vectors pSV-1 and pSV-2. Comparable to pM-induced MMP-2 knockdown, pM-1 and pM-2 treatments also resulted in a noticeable decrease in proliferation compared to respective pSV-1 and pSV-2 controls (Supplementary Fig. S3A). The conditioned media from pM-1 and pM-2 treated cells showed drastic reduction in the secreted levels of IL-6, IL-8 and IL-10 in corroboration with the downregulation of cellular expression levels of α5 integrin, β1 integrin, IL-6, phospho-Stat3, (Supplementary Fig. S3B, S3C). The effect of MMP-2 downregulation was also evaluated in another two human glioma cell lines, U251 and U87, which confirmed the noticeable decrease in proliferation and suppression of α5, β1, IL-6, expression and JAK1, JAK2 and Stat3 phosphorylation levels (Supplementary Fig. S4).

IL-6 mediates pM-induced inhibition of constitutive Stat3 activation

To further evaluate the significance of MMP-2.siRNA-induced IL-6 inhibition on subsequent JAK/Stat3 pathway attenuation, we overexpressed IL-6 and confirmed the enhanced mRNA and protein expression levels of IL-6 in transfected 4910 and 5310 cells after 24 hours (Supplementary Fig. S5A). There was remarkable elevation of gp130, phopsho-JAK1, JAK1, phospho-JAK2, JAK2 and phospho-Stat3 expression levels in cells treated with pIL-6 alone or pSV+pIL-6 compared to either mock- or pSV-treated cells. In contrast the expression levels of IL-6, phospho-JAK2, and phosho-Stat3 in pM+IL-6 treatments were elevated when compared to pM treatment alone and lesser in comparison to either pIL-6 or pSV+pIL-6 treatments, implying a significant reversal of phospho-Stat3 inhibition by IL-6 overexpression in pM-treated cells. The reversal in gp130, phospho-JAK1, JAK1, phospho-JAK2, JAK2 and phospho-Stat3 expression correlated with IL-6 overexpression in pM-treated cells, further implying that the MMP-2 depletion attenuated the IL-6-mediated Stat3 activation (Figure 5A). Corroborating previous reports showing MMP-2 as a potential Stat3 target gene, IL-6 overexpression in turn resulted in remarkable elevation in MMP-2 gelatinolytic activity, which was suppressed in pM+pIL-6 combination treatment (Supplementary Figure S5B). Additionally, EMSA also showed significant reversal of IL-6-induced Stat3-DNA binding activity in pM+pIL-6 treatment suggesting that the loss of MMP-2 activity inhibited the IL-6 mediated Stat3 activation (Figure 5B). Confocal microscopy also revealed elevation in phospho-Stat3 nuclear localization in pIL-6-treated cells compared to mock-treated cells and pM+pIL-6-treated cells showed an expression pattern similar to either mock or pSV treatment confirming the reversal of pM-inhibited phospho-Stat3 nuclear localization in pIL-6-treated cells (Supplementary Figure S5C). The effect of pM and pM+pIL-6 treatments was further checked on cell proliferation using BrDU assay. IL-6 overexpression restored the pM-inhibited proliferation in pM+pIL-6 treatment (Figure 5C). Additionally, we observed a consistent reversal in pM-induced PARP and caspase-3 cleavage, and inhibition in CyclinD1 and c-Myc expression levels in pM +pIL-6-treated cells, which directly indicates that the loss of MMP-2 leads to the suppression of IL-6/Stat3 proliferation signaling (Figure 5D).

Overexpression of siRNA-insensitive MMP-2 or supplementation of rhMMP-2 counteracts pM-induced Stat3 suppression and apoptosis

To establish specificity of pM-inhibited IL-6/Stat3 activation and to avoid any off-target consequences, we treated mock-, pSV- and pM-treated cells with siRNA-insensitive MMP-2 overexpression plasmid (pM-FL-A141G) or rhMMP-2 as described in Materials and Methods. The expression levels of α5, β1, phospho-Stat3, CyclinD1 and c-Myc were elevated in both pM-FL-A141G and rhMMP-2 treated cells, implicating a possible role of MMP-2 in the regulation of the α5β1-mediated Stat3 activation and cell proliferation (Figure 6A). As shown in Fig. 6B, the loss-and-gain of function approach by pM and pM-FL-A141G or rhMMP-2 treatments showed a significantly enhanced MMP-2/α5β1 association by complex formation in rhMMP-2- or pM-FL-A141G-treated cells and decreased association in pM-treated cells. Immunoprecipitation with non-specific (Nsp-IgG) did not show precipitation and re-probing the IP blots with anti-α5, anti-β1 and anti-Myc antibodies further confirmed the band specificity. Densitometric analysis of relative binding confirmed that the pM+rhMMP-2 or pM+pM-FL-A141G combination treatment noticeably counteracted the rhMMP-2- or pM-FL-A141G-elevated MMP-2/α5β1 binding, which further evidences direct substantial MMP-2/α5β1 integrin interaction in both 4910 and 5310 cells. In correlation with MMP-2 overexpression-induced MMP-2/α5β1 binding, EMSA displayed obvious elevation in Stat3 DNA-binding activity in rhMMP-2 treatment which is reduced in pM+rhMMP-2-treated cells confirming the role of MMP-2 in maintaining constitutive Stat3 activity (Figure 6C). A noticeable elevation in Stat3 occupancy on to CylcinD1 and c-Myc promoters was observed in pM-FL-A141G- or rhMMP-2-treated 4910 and 5310 cells. In corroboration with the reversal of MMP-2/α5β1 complex formation in pM +rhMMP-2 and pM+pM-FL-A141G treated cells, a clear reversal in Stat3 promoter recruitment was observed suggesting a role of MMP-2 in α5β1-mediated Stat3 activation and promoter binding (Figure 6D). Additionally, the pM-induced loss of cell proliferation was reversed in pM+rhMMP-2 or pM+pM-FL-A141G treatments whereas individual rhMMP-2 or pM-FL-A141G treatments alone enhanced the proliferation rate in both cell lines indicating the role of MMP-2 in maintenance of tumor cell proliferation (Figure 6E).

Blocking α5β1 Integrin negated the rhMMP-2-induced IL-6/Stat3 activation

To further assess the pM-inhibited α5β1 signaling, we elevated the β1 signaling by FN adhesion in mock-, pSV- and pM-treated cells. Western blotting indicated the α5β1-mediated elevation in phospho-Stat3, CyclinD1 and c-Myc expression levels were decreased in pM-treated cells evidencing the role of MMP-2 in the regulation of α5β1-mediated Stat3 activation (Figure 7A). The essential functional role of MMP-2/α5β1 interaction on rhMMP-2-induced and pM-inhibited activation of IL-6/Stat3 was verified by treating the cells with α5β1 blocking antibody in combination with pM and rhMMP-2 treatments. The effect of α5β1 blocking antibody on pM-inhibited IL-6/Stat3 activation and subsequent cell survival was checked to investigate the role of MMP-2/α5β1 coupling in these tumor cell lines. Blocking of α5β1 integrin further reduced the pM-inhibited recruitment of Stat3 on both CyclinD1 and c-Myc promoters suggesting the functional significance of MMP-2 and α5β1 integrin co-operativity (Figure 7B). Supplementation of α5β1 blocking antibody to rhMMP-2-treated 4910 and 5310 cells substantially decreased the rhMMP-2-induced expression levels of IL-6, phospho-Stat3, CyclinD1 and c-Myc. On the other hand,

augmentation of α5β1 blocking antibody to pM-treated cells further decreased the pM-inhibited expression levels of IL-6, phopsho-Stat3, CyclinD1 and c-Myc expression levels implying the significance of MMP-2 binding in α5β1-mediated Stat3 activation and cell survival. The expression levels of Stat3 target proteins CyclinD1 and c-Myc were severely reduced and almost undetectable in pM+anti-α5β1 integrin treatments in both the cell lines when compared to either pM- or anti-α5β1 integrin-treatments indicating that the loss of MMP-2 augments the inhibitory effects of α5β1 blocking antibody (Figure 7C). The combination of pM and α5β1 substantially inhibited the rhMMP-2-induced Stat3 activation and expression of CyclinD1 and c-Myc proteins when compared to either pM or anti-α5β1 treatments alone, which indicates that the disruption of MMP-2 and α5β1 association inhibits IL-6/Stat3 survival signaling leads to decrease in proliferation in 4910 and 5310 glioma xenograft cells.

pM-inhibited intracranial tumor growth in athymic mice

In vivo experiments showing the effect of pM-treatment on intracranial tumor growth by orthotropic injection of 4910 and 5310 cells showed remarkable decrease in the tumor size when compared to mock- and pSV-treated tumors (Figure 8A). High expression and predominant co-localization MMP-2 and α5β1 integrin at membrane periphery were identified in both mock- and pSV-treated tumors (Figure 8B). In contrast, pM-treated tumors showed substantial decrease in MMP-2 and α5β1 expression, which subsequently led to decreased MMP-2/α5β1 co-localization correlating with reduced IL-6 and phospho-Stat3 expression levels (Figure 8C). Further expression levels of proliferation markers Ki-67 and PCNA were studied to check the number of proliferating cells in sections which revealed the severely inhibition Ki-67 and PCNA positivity in pM-treated tumor sections whereas the mock- and pSV- treated control tumors showed high proliferating cells with intense nuclear Ki-67 and PCNA staining (Supplementary Figure S6). The CyclinD1 and c-Myc expression was significantly decreased in pM-treated tumor sections when compared to pSV-treated control counterparts (Supplementary Figure S7). These *in vivo* observations corroborate the *in vitro* findings confirming the role of MMP-2 in α5β1 mediated IL-6/Stat3 signaling activation in glioma.

DISCUSSION

Apoptotic cell death plays a crucial role in the development of multi-cellular organisms, but it is also a major concern in cancer treatment as cancer is a consequence of aberrant cell proliferation there by manipulation of the extra- and intracellular signals directing intracellular oncogenic signaling activation may serve to drive tumor cells towards cell death (39). MMPs are the extracellular matrix remodeling proteases that act as critical mediators in tumor microenvironment changes (2). Integrins are membrane-spanning proteins, with their extracellular domains bound to the ECM proteins while their cytoplasmic tails facilitate assembly of intracellular proteins and propagate the outside-in signaling. Among other integrins, accumulating evidences indicate the high expression of α5β1 in glioblastoma cells suggesting its potential as a new therapeutic target (37, 40). One of the key mechanisms of integrins is their interaction and modulation of MMP activity (16, 17). The α5β1 integrin activates NF-κB proliferative signaling and elevates the expression

of genes involved in angiogenesis and inflammation whereas Chinese hampster ovary (CHO) cells expressing truncated α5Δcβ1 without the cytoplasmic domain show impaired NF-κB activation, leading to cell death (13, 41). In a recent report, Shain *et al.* (42) demonstrated the role of β1 integrin in IL-6 mediated Stat3 survival signaling in multiple myeloma cells. Studies on the blockade of the IL-6/Stat3 signaling pathway by anti-IL-6 receptor antibody substantially inhibited tumor progression by downregulating Stat3 signaling in human colon carcinoma cells (43). Targeting β1 integrins with β1-inhibitory antibody significantly inhibits proliferation by apoptosis in breast cancer cells *in vitro* and *in vivo* (44). A non-RGD-based peptide inhibitor of α5β1 integrin ATN-161 and a functional blocking α5β1 integrin antibody blocks *in vivo* tumor growth and metastasis in breast cancer cells (45). The N-glycosylation of Interaction-like (I-like) domain of β1 integrin is required for α5β1 heterodimer formation, and the role of α5β1 in tumor cell survival signaling has been elucidated previously (12, 13, 38, 46). On the other hand, the α5β1 integrin functional blocking inhibitory antibody Volociximab significantly reduced tumor growth in mouse and rabbit VX2 carcinoma models (47).

Though several studies suggested the effect of various integrins on the manipulation of cytokine levels, the effect of α5β1 integrin heterodimer on IL-6 expression and its downstream signaling is unknown. A functional significance of the MMP-2/β1 integrin binding was confirmed by immunoprecipitation in the negative regulation of human endothelial cell apoptosis has been reported earlier (48). Association between MMP-2 and α5β1 integrin by direct binding in melanoma and breast cancer cells and co-localization of MMP-2/α5β1 in migrating astrocytes has been indicated previously (16–18). Based on these reports, we sought to determine whether there was any direct interaction of MMP-2/α5β1 integrin by complex formation in glioma. Here, for the first time, we show significant interaction of MMP-2 with α5β1 heterodimer in human glioma xenograft cells both *in vitro* and *in vivo*. However, our co-immunoprecipitation and co-localization studies do not show direct binding between MMP-2 and α5β1 integrin but indicate that they form a complex which may be bridged by unidentified proteins. Recent reports showed the effect of NF-κB blockade on inhibition of cancer cell adhesion via downregulation of α2, α3 and β1 integrins (49). Previous studies on MMP-2 knockdown showed inhibition of NF-κB nuclear localization and DNA-binding activity (50). Our present studies showing pM-inhibited β1 integrin transcriptional and protein expression suggest a possible indirect role of pM-inhibited NF-κB in the downregulation of these integrin molecules. The role of β1 integrin in enhancing IL-6 mediated Stat3 signaling in multiple myeloma has been previously elucidated (42). Role of IL-6 in JAK/Stat3-mediated MMP-2 activation in pancreatic and glioma cancer cells and MMP-10 activation in lung adenocarcinoma cells has been reported to enhance growth and invasion (32, 51, 52). Farber, *et al*. (37) showed that the treatment with α5β1 integrin inhibitor JSM6427 does not have any effect on the cytokine release pattern in microglial cells. However, in our studies with glioma xenograft cell lines, the MMP-2 siRNA-mediated inhibition of α5β1 expression is in correlation with changes in the cytokine release pattern in 4910 and 5310 cells, suggesting the effects of α5β1 inhibition are cell-specific. The significance of IL-6 in tumor progression has been reported (53, 54). The specific role of MMP-2 downregulation on inhibition of α5, β1, IL-6 expression and Stat3 phosphorylation were further confirmed by employing 3 different MMP-2.siRNAs and this

effect was also checked in U251 and U87 human glioma cell lines. Our studies with α5β1 blocking by functional blocking antibody paralleled with the effect of MMP-2 downregulation inhibiting IL-6 expression and hindered Stat3 phosphorylation and recruitment on to Cyclin D1 and c-Myc promoters indicates high relevance to MMP-2/α5β1 interaction in maintaining IL-6 mediated constitutive Stat3 activation in glioma. The significant inhibition of α5β1-mediated IL-6/Stat3 activation in MMP-2 downregulation was further analyzed *in vivo* which indicated significant reduction in IL-6, phospho-Stat3 levels leading to reduced tumor growth. Suppression of IL-6 and IL-8, target genes of NF-κB in MMP-2 siRNA treatment in both cell lines, is in parallel with our previous observation of decreased NF-κB activation upon MMP-2 downregulation in both 4910 and 5310 cell lines (50). Our observations on α5β1 role in the activation of IL-6 mediated Stat3 signaling activation in glioma xenograft cells also corroborate previous reports on the role of α5β1 integrin adhesion in elevating the IL-6-mediated STAT3 pathway in multiple myeloma cells (42).

In summary, our findings on MMP-2.siRNA mediated α5β1 suppression in two human xenograft cell lines 4910 and 5310, imply that role of MMP-2 in the regulation α5β1 mediated cellular signaling. The study provides further insights in to the co-operativity between MMP-2 and α5β1 integrin by indirect physical interaction in the maintenance of constitutive IL-6 mediated Stat3 DNA-binding activity and expression of subsequent downstream effector genes suggesting MMP-2 suppression as a potential therapeutic approach in glioma treatment.

MATERIALS AND METHODS

Cells, reagents and antibodies

Human glioma xenograft cell lines 4910 and 5310 (kindly provided by Dr. David James, University of California, San Francisco) are highly invasive in mouse brain were developed and maintained in mice (55). These cells were cultured in RPMI 1640 (Mediatech Inc., Herndon, VA) medium supplemented with 10% fetal bovine serum (Invitrogen Corporation, Carlsbad, CA), 50 units/mL penicillin, and 50 μg/mL streptomycin (Life Technologies, Inc., Frederick, MD) by incubation in a humidified 5% CO_2 chamber at 37°C. Human glioma cell lines U251 and U87 (American Type Culture Collection) were grown in RPMI medium 1640 containing glutamate (5mM) and 5% FBS and maintained in CO_2 incubator. We used antibodies against MMP-2, IL-6, IL-8, IL-10, α5-integrin, β1-integrin, phospho-JAK1 (Tyr1022), phospho-JAK2 (Tyr1007/1008), gp130, Stat3 (sc-482 X; Gel supershift & ChIP grade), phopsho-Stat3 (Tyr705), phospho-Stat3 (Ser727), c-Myc, CyclinD1, Bcl-x(L), Bcl-2, Survivin, Ki-67, PCNA, GAPDH, and HRP/Alexa Fluor® conjugated secondary antibodies (Santa Cruz Biotechnology, Santa Cruz, CA), caspase-3 and poly (ADP-ribose) polymerase (Cell Signal Technology). Anti-integrin α5β1, clone HA5 (MAB1999), and α5β1 functional blocking antibody (MAB1969) (Millipore Inc., Billerica, MA) were obtained. Human Brain Tumor Tissue Microarray, GL2082 (US Biomax, Inc, Rockville, MD), IL-6 overexpression (pIL-6) plasmid (Origene technologies, Rockville, MD) and human recombinant-MMP-2 protein (rhMMP-2) were also purchased for this study (EMD Biosciences, San Diego, CA).

Construction of siRNA-insensitive plasmid and transient transfection treatments

Transient transfection studies were performed as described previously by Kesanakurti *et al.* (50). In brief, cells were transfected with pcDNA3.0 containing MMP-2.siRNA sequence (pM, targets 131–152 nucleotides of MMP-2 cDNA) and specific scrambled siRNA sequence (pSV) cloned as described previously (50) using FuGene HD transfection reagent following manufacturer's instructions (Roche Applied Science, Indianapolis, IN). The effect of MMP-2 downregulation was also checked by transient transfection studies using MMP-2.siRNA-1 (pM-1 [caaatatgagagctgcaccag], pcDNA3.0 vector containing siRNA targeting 1073–1094 nucleotides in MMP-2 cDNA) and MMP-2.siRNA-2 (pM-2 [pool of siRNAs targeting different regions of MMP-2, sc-29398], purchased from Santa Cruz Biotechnology, Santa Cruz, CA) in comparison to specific scrambled vectors pSV-1 and pSV-2. Full-length cDNA of MMP-2 was RT-PCR amplified using sequence specific primers and cloned in *Eco*RI and *Xba*I sites of pcDNA3.1(+)/myc-His-A (Invitrogen Corporation, Carlsbad, CA) to construct overexpression plasmid (pM-FL). A silent mutation was introduced within the siRNA-targeted MMP-2 cDNA sequence (nucleotides 131–152, 5'-AACGGACAA**A**GAGTTGGCAGT-3') without changing the aminoacid sequence (nucleotides 131–152, 5'-AACGGACAA**G**GAGTTGGCAGT-3') by using pM-FL as a template and QuickChange site-directed mutagenesis kit (Stratagene, La Jolla, CA, USA) following manufacturer's instructions. This siRNA-insensitive plasmid with A141G mutation was verified by DNA sequencing and is designated as pM-FL-A141G. For combination treatments, at 24 h post-transfection with mock (1×PBS), pSV or pM, cells were further transfected with pIL-6 or pM-FL-A141G or recombinant human MMP-2 (rhMMP-2; 25 ng/mL) or α5β1 blocking antibody (10 μl/mL) were added to the medium and cells were incubated for another 24 h. The β1 integrin activation by Fibronectin (FN) adhesion was achieved by detaching the mock-, pSV- and pM-treated cells by trypsinization after 24 h of transfection and re-plating them on FN-coated culture plates and cells were incubated for another 24 h.

Semi-quantitative and quantitative PCR and PCR array

Total RNA was isolated using TRIzol reagent (Invitrogen, Carlsbad, CA) following manufacturer's instructions. cDNA was synthesized from 2 μg of total RNA using ImProm-II Reverse Transcription kit (Promega Corporation, Madison, WI). Semi-quantitative PCR was performed using the following set of primers: MMP-2 sense 5'-GTGCTGAAGGACACACTAAAGA-3' and MMP-2 antisense 5'-CCTACAACTTTGAGAAGGATGGCAA-3'; IL-6 sense 5'-GAACTCCTTCTCCACAAG-3' and IL-6 antisense 5'-CTGAAGAGGTGAGTGGCTG-3'; GAPDH sense 5'-GGAGTCAACGGATTTGGTCGTAT-3' and GAPDH antisense 5'-GTCTTCACCACCATGGAGAAGGCT-3' respectively. PCR array was performed using Human JAK/STAT Signaling Pathway RT^2 Profiler™ PCR Array kit following manufacturer's instructions (SA Biosciences, Frederick, MD). This array comprises all Stat3 signaling family members including receptors, nuclear co-factors, and co-activators associated with the Stat proteins, STAT-inducible genes, and regulators of STAT pathway. Following PCR conditions using 1 μL of cDNA template were used: 1 cycle of 95°C 10 min and 40 cycles of 95 °C 15 s, 60 °C 30 s, 72 °C 30 s, followed by 1 cycle of 72°C 10 min.

Data obtained from three experimental replicates were analyzed using iCycler IQ version 3.1 software (Bio-Rad) and Ct values were converted into fold change, using web-based analysis software (http://pcrdataanalysis.sabiosciences.com/pcr/arrayanalysis.php).

ChIP assay

Chromatin immunoprecipitation assays was performed using ChIP-IT™ Express Magnetic Chromatin Immunoprecipitation kit following manufacturer's protocol (Active motif, Carlsbad, CA). Briefly, cells were fixed in 37% formaldehyde, and chromatin was sheared by sonication and immunoprecipitated using anti-Stat3 and Normal sheep IgG antibodies by incubation at 4°C for 2–4 hours on a rotor. The immunoprecipitates was collected by using magnetic protein G beads (Millipore, Temecula, CA), which were washed thoroughly to remove non-specific DNA binding. The chromatin was eluted from the beads, and cross-links were removed by overnight incubation at 65°C. DNA was then purified from the beads using the chelating resin solution and about 10 ng of immunoprecipitated DNA was used to detect Stat3 binding to CyclinD1 and c-Myc promoter sequences by standard PCR. The following ChIP primers were used for c-Myc-sense-5'-GAAGCCTGAGCAGGCGGGGCAGG-3'; c-Myc-antisense-5'-GCTTTGATCAAGAGTCCCAG-3' and CyclinD1-sense-5'-AACTTGCACAGGGGTTGTGT-3'; CyclinD1-antisense-5'-GAGACCACGAGAAGGGGTGACTG-3' respectively. The amplification was maintained in a linear range by performing PCR with a serial dilution of input and various cycles (30–40 cycles). Pre-immunoprecipitated input DNA represents 5% of total chromatin used in each reaction before immunoprecipitation. Primers specific to GAPDH, 5'-CGGTGCGTGCCCAGTTG-3' and 5'-GCGACGCAAAAGAAGATG-3' were used for PCR amplification of input samples as a control to monitor equal loading and non-specific IgG immunoprecipitates were also loaded (negative control) as described previously (56). The amplification products were resolved on 2% ethidium bromide agarose gels and visualized under UV light and data represents three experimental replications.

Western blotting and immunoprecipitation

Western blotting and immunoprecipitation studies were performed as described previously by Kesanakurti et al. (57). Shortly, whole cell lysates were isolated using radioimmunoprecipitation assay (RIPA) buffer and equal amounts of protein were resolved over SDS-PAGE and transferred on to PVDF membrane. Blots were incubated in respective primary and HRP-conjugated secondary antibodies followed by detection using an enhanced chemiluminescence kit (Pierce Biotechnology, Rockford, IL). Equal amounts of protein (200μg) were immunoprecipitated with antibodies against MMP-2, α5, β1, α5β1 and non-specific IgG using μMACS™ protein G microbeads and MACS separation columns following manufacturer's protocol and immunoprecipitates were subjected to western blotting.

Gelatin zymography and cytokine array

Gelatin zymographic analyses and cytokine array using tumor conditioned media (CM) were performed as described previously (50). Briefly, medium was aspirated from culture plates at 36 h post-transfection, 3 mL of serum-free medium was added and incubated for another

12 h at the end of which tumor-conditioned media (CM) containing the secretory proteins, cytokines and various growth factors was collected. CM was resolved over 0.1% gelatin containing SDS-polyacrylamide gels. Subsequently, gels were washed with 2.5% Triton X-100 to remove SDS, followed by 16- to 20-hour incubation at 37°C in Tris-$CaCl_2$ buffer (pH 7.6), stained with Coomassie brilliant blue (0.25%) and destained to visualize the gelatinolytic activity. Cytokine array to detect the secretory levels of various cytokines present in the tumor conditioned media obtained from pSV- and pM-treated cells was performed using a Human Cytokine Array 3 kit following the manufacturer's instructions (Ray Biotech®, Norcross, GA). The average signal intensity of each cytokine dotted in duplicate on the array was estimated in three independent experimental replicates and denoted as mean±SE while biotin-conjugated and unconjugated IgG signals represented positive and negative signals in the analysis.

Electrophoretic mobility shift assay (EMSA)

Nuclear proteins were isolated using Biovision Nuclear/Cytosol fractionation Kit (Mountain View, CA) following manufacturer's protocol. EMSA for STAT3 DNA-binding activity was performed using Panomics EMSA Kit (Panomics, Inc. Fremont, CA) as described by Kesanakurti *et al.* (50). In brief, nuclear extracts (2×10^6 cells) from different treatments were allowed to bind with biotin-end-labeled DNA in the presence of 2×binding buffer and poly dI-dC (deoxyinosinic-deoxy-cytidylic acid) by incubation at 15°C for 30 min. These DNA-protein complexes were subjected to native gel electrophoresis and transferred onto Hybond-N^+ membrane (Amersham, Piscataway, NJ). After transfer, DNA was UV cross-linked, and activity was detected by binding with streptavidin-HRP conjugate and chemiluminescent substrate.

Cell proliferation (BrDU) and Clonogenic assay

Proliferation rate in cells was determined by BrDU assay (Roche Applied Science, IN, USA) measuring the incorporation of pyrimidine analogue, 5-bromo-2'-deoxyuridine (BrDU) during DNA synthesis. Briefly, cells were plated in 96-microwell plates, incubated overnight and subjected to different treatments as described above. Colorimetric estimation of BrDU incorporation was carried out by quantification of antibody-peroxidase reaction product at dual wavelengths of 450/540 nm using multiwell spectrophotometer as described by Ganji *et al.* (58). Percentage of BrDU incorporation was compared to mock-treated cells (100%) and represented as mean±SE values obtained in at least three independent experiments. Mono-layer colony formation assay was performed as described previously (59). In short, about ~0.5×10^3 cells were seeded in 100 mm plates and different treatments were carried out in triplicate as described above and cells were continued to culture for 10 days to allow colony formation. Hema-3 stained colonies were counted under light microscope to estimate the percentage of colony formation in different treatments.

Immunocytochemical and immunohistochemical analyses

Immunocytochemical and immunohistochemical analyses were performed as described earlier (50). Briefly, after treatments cells in chamber slides were fixed, permeabilized and incubated with respective primary and Alexa Fluor®-conjugated secondary antibodies and

subsequently mounted. For nuclear counterstaining, 4'-6-diamidino-2-phenylindole (DAPI) was used. For immunohistochemical analysis, de-paraffinized tissue sections (4–5 μm) were blocked in 3% BSA in 1×PBS and incubated overnight at 4°C with respective primary antibodies followed by incubation with Alexa Fluor®/HRP-conjugated secondary antibodies for 1 hour at room temperature. Sections were subsequently counterstained with DAPI, mounted and observed under confocal microscope. For DAB (3,3'-Diaminobenzidine) staining, hematoxylin was used for nuclear staining, mounted and pictured under light microscope.

In vivo experiments

4910 and 5310 cells (1×10^6 cells per mouse) were injected sterotactically into 4-6-week old female *nu/nu* mice to establish tumor growth as described earlier (50). Tumors were allowed to grow for ten days, the animals were divided into three sets (n=10) and Alzet osmotic pumps (model 2004, ALZET Osmotic Pumps, Cupertino, CA) were implanted for plasmid delivery (dose: 6–8 mg/kg body weight). Brains were excised after 60 days, fixed, paraffinized and the tumor area from every fifth Hematoxylin & Eosin (H&E) stained tumor section was manually estimated with the aid of a microscope attached to a computer screen, using Image Pro Discovery Program software (Media Cybernatics, Inc., Silver Spring, MD). The tumor volumes were then calculated as summed tumor area on all sections multiplied by width of the sections and plotted as mean±SE obtained from a group of ten animals.

Statistical analysis

Data obtained from different sets of treatments were evaluated with one-way ANOVA using Neumann-Keuls method of Sigmastat 3.1. Densitometric analysis was performed using ImageJ 1.42 software (NIH) and data are represented in the form of mean±SE obtained from at least three independent repetitions. Significant difference among different treatment groups was denoted by * at $p\leq0.05$ and ** at $p\leq0.01$.

Supplementary Material

Refer to Web version on PubMed Central for supplementary material.

ACKNOWLEDGEMENTS

We thank Shellee Abraham for manuscript preparation and Diana Meister and Sushma Jasti for manuscript review.

Funding: This research was supported by award NS64535-01A2 (to J.S.R.) from the National Institute of Neurological Disorders and Stroke.

Reference List

1. Louis DN. Molecular pathology of malignant gliomas. Annu Rev Pathol. 2006; 1:97–117. [PubMed: 18039109]
2. Kessenbrock K, Plaks V, Werb Z. Matrix metalloproteinases: regulators of the tumor microenvironment. Cell. 2010; 141:52–67. [PubMed: 20371345]
3. Rao JS. Molecular mechanisms of glioma invasiveness: the role of proteases. Nat Rev Cancer. 2003; 3:489–501. [PubMed: 12835669]

4. Chang C, Werb Z. The many faces of metalloproteases: cell growth, invasion, angiogenesis and metastasis. Trends Cell Biol. 2001; 11:S37–S43. [PubMed: 11684441]
5. Han X, Nabors LB. Integrins-a relevant target in glioblastoma. Eur J Clin & Med Oncol. 2010; 2:59–64.
6. Brooks PC, Stromblad S, Sanders LC, von Schalscha TL, Aimes RT, Stetler-Stevenson WG, et al. Localization of matrix metalloproteinase MMP-2 to the surface of invasive cells by interaction with integrin alpha v beta 3. Cell. 1996; 85:683–693. [PubMed: 8646777]
7. Chetty C, Lakka SS, Bhoopathi P, Rao JS. MMP-2 alters VEGF expression via aVB3 integrin-mediated PIK/AKT signaling in A549 lung cancer cells. Int J Cancer. 2010; 127:1081–1095. [PubMed: 20027628]
8. Morgan MR, Thomas GJ, Russell A, Hart IR, Marshall JF. The integrin cytoplasmic-tail motif EKQKVDLSTDC is sufficient to promote tumor cell invasion mediated by matrix metalloproteinase (MMP)-2 or MMP-9. J Biol Chem. 2004; 279:26533–26539. [PubMed: 15067014]
9. Silletti S, Kessler T, Goldberg J, Boger DL, Cheresh DA. Disruption of matrix metalloproteinase 2 binding to integrin alpha vbeta 3 by an organic molecule inhibits angiogenesis and tumor growth in vivo. Proc Natl Acad Sci USA. 2001; 98:119–124. [PubMed: 11134507]
10. Aoudjit F, Vuori K. Integrin signaling inhibits paclitaxel-induced apoptosis in breast cancer cells. Oncogene. 2001; 20:4995–5004. [PubMed: 11526484]
11. Courter DL, Lomas L, Scatena M, Giachelli CM. Src kinase activity is required for integrin alphaVbeta3-mediated activation of nuclear factor-kappaB. J Biol Chem. 2005; 280:12145–12151. [PubMed: 15695822]
12. Korah R, Boots M, Wieder R. Integrin alpha5beta1 promotes survival of growth-arrested breast cancer cells: an in vitro paradigm for breast cancer dormancy in bone marrow. Cancer Res. 2004; 64:4514–4522. [PubMed: 15231661]
13. Lee BH, Ruoslahti E. alpha5beta1 integrin stimulates Bcl-2 expression and cell survival through Akt, focal adhesion kinase, and Ca2+/calmodulin-dependent protein kinase IV. J Cell Biochem. 2005; 95:1214–1223. [PubMed: 15962308]
14. Matter ML, Ruoslahti E. A signaling pathway from the alpha5beta1 and alpha(v)beta3 integrins that elevates bcl-2 transcription. J Biol Chem. 2001; 276:27757–27763. [PubMed: 11333270]
15. Mitra A, Chakrabarti J, Chatterjee A. Binding of alpha5 monoclonal antibody to cell surface alpha5beta1 integrin modulates MMP-2 and MMP-7 activity in B16F10 melanoma cells. J Environ Pathol Toxicol Oncol. 2003; 22:167–178. [PubMed: 14529092]
16. Morozevich G, Kozlova N, Cheglakov I, Ushakova N, Berman A. Integrin alpha5beta1 controls invasion of human breast carcinoma cells by direct and indirect modulation of MMP-2 collagenase activity. Cell Cycle. 2009; 8:2219–2225. [PubMed: 19617714]
17. Morozevich GE, Kozlova NI, Cheglakov IB, Ushakova NA, Preobrazhenskaya ME, Berman AE. Implication of alpha5beta1 integrin in invasion of drug-resistant MCF-7/ADR breast carcinoma cells: a role for MMP-2 collagenase. Biochemistry (Mosc). 2008; 73:791–796. [PubMed: 18707587]
18. Ogier C, Bernard A, Chollet AM, LE DT, Hanessian S, Charton G, et al. Matrix metalloproteinase-2 (MMP-2) regulates astrocyte motility in connection with the actin cytoskeleton and integrins. Glia. 2006; 54:272–284. [PubMed: 16845676]
19. Dranoff G. Cytokines in cancer pathogenesis and cancer therapy. Nat Rev Cancer. 2004; 4:11–22. [PubMed: 14708024]
20. Hong DS, Angelo LS, Kurzrock R. Interleukin-6 and its receptor in cancer: implications for Translational Therapeutics. Cancer. 2007; 110:1911–1928. [PubMed: 17849470]
21. Salgado R, Junius S, Benoy I, Van Dam P, Vermeulen P, Van Marck E, et al. Circulating interleukin-6 predicts survival in patients with metastatic breast cancer. Int J Cancer. 2003; 103:642–646. [PubMed: 12494472]
22. Song L, Rawal B, Nemeth JA, Haura EB. IL6/JAK1 pathway inhibition downregulates STAT3 and inhibits tumor growth in lung cancer. Mol Cancer Ther. 2011; 10:481–494. [PubMed: 21216930]

23. Wang H, Lathia JD, Wu Q, Wang J, Li Z, Heddleston JM, et al. Targeting interleukin 6 signaling suppresses glioma stem cell survival and tumor growth. Stem Cells. 2009; 27:2393–2404. [PubMed: 19658188]
24. Weissenberger J, Loeffler S, Kappeler A, Kopf M, Lukes A, Afanasieva TA, et al. IL-6 is required for glioma development in a mouse model. Oncogene. 2004; 23:3308–3316. [PubMed: 15064729]
25. Bollrath J, Greten FR. IKK/NF-kappaB and STAT3 pathways: central signalling hubs in inflammation-mediated tumour promotion and metastasis. EMBO Rep. 2009; 10:1314–1319. [PubMed: 19893576]
26. Bollrath J, Phesse TJ, von BV, Putoczki T, Bennecke M, Bateman T, et al. gp130-mediated Stat3 activation in enterocytes regulates cell survival and cell-cycle progression during colitis-associated tumorigenesis. Cancer Cell. 2009; 15:91–102. [PubMed: 19185844]
27. Bowman T, Broome MA, Sinibaldi D, Wharton W, Pledger WJ, Sedivy JM, et al. Stat3-mediated Myc expression is required for Src transformation and PDGF-induced mitogenesis. Proc Natl Acad Sci USA. 2001; 98:7319–7324. [PubMed: 11404481]
28. Grandis JR, Drenning SD, Zeng Q, Watkins SC, Melhem MF, Endo S, et al. Constitutive activation of Stat3 signaling abrogates apoptosis in squamous cell carcinogenesis in vivo. Proc Natl Acad Sci USA. 2000; 97:4227–4232. [PubMed: 10760290]
29. Levy DE, Inghirami G. STAT3: a multifaceted oncogene. Proc Natl Acad Sci USA. 2006; 103:10151–10152. [PubMed: 16801534]
30. Xiong H, Zhang ZG, Tian XQ, Sun DF, Liang QC, Zhang YJ, et al. Inhibition of JAK1, 2/STAT3 signaling induces apoptosis, cell cycle arrest, and reduces tumor cell invasion in colorectal cancer cells. Neoplasia. 2008; 10:287–297. [PubMed: 18320073]
31. Curran S, Murray GI. Matrix metalloproteinases: molecular aspects of their roles in tumour invasion and metastasis. Eur J Cancer. 2000; 36:1621–1630. [PubMed: 10959048]
32. Huang C, Yang G, Jiang T, Huang K, Cao J, Qiu Z. Effects of IL-6 and AG490 on regulation of Stat3 signaling pathway and invasion of human pancreatic cancer cells in vitro. J Exp Clin Cancer Res. 2010; 29:51. [PubMed: 20482858]
33. Xie TX, Wei D, Liu M, Gao AC, Ali-Osman F, Sawaya R, et al. Stat3 activation regulates the expression of matrix metalloproteinase-2 and tumor invasion and metastasis. Oncogene. 2004; 23:3550–3560. [PubMed: 15116091]
34. Rahaman SO, Harbor PC, Chernova O, Barnett GH, Vogelbaum MA, Haque SJ. Inhibition of constitutively active Stat3 suppresses proliferation and induces apoptosis in glioblastoma multiforme cells. Oncogene. 2002; 21:8404–8413. [PubMed: 12466961]
35. Senft C, Priester M, Polacin M, Schroder K, Seifert V, Kogel D, et al. Inhibition of the JAK-2/STAT3 signaling pathway impedes the migratory and invasive potential of human glioblastoma cells. J Neurooncol. 2011; 101:393–403. [PubMed: 20589525]
36. Chetty C, Bhoopathi P, Joseph P, Chittivelu S, Rao JS, Lakka SS. Adenovirus-mediated siRNA against MMP-2 suppresses tumor growth and lung metastasis in mice. Mol Cancer Ther. 2006; 5:2289–2299. [PubMed: 16985063]
37. Farber K, Synowitz M, Zahn G, Vossmeyer D, Stragies R, Van Rooijen N, et al. An alpha5beta1 integrin inhibitor attenuates glioma growth. Mol Cell Neurosci. 2008; 39:579–585. [PubMed: 18804537]
38. Maglott A, Bartik P, Cosgun S, Klotz P, Ronde P, Fuhrmann G, et al. The small alpha5beta1 integrin antagonist, SJ749, reduces proliferation and clonogenicity of human astrocytoma cells. Cancer Res. 2006; 66:6002–6007. [PubMed: 16778170]
39. Melet A, Song K, Bucur O, Jagani Z, Grassian AR, Khosravi-Far R. Apoptotic pathways in tumor progression and therapy. Adv Exp Med Biol. 2008; 615:47–79. [PubMed: 18437891]
40. Martinkova E, Maglott A, Leger DY, Bonnet D, Stiborova M, Takeda K, et al. alpha5beta1 integrin antagonists reduce chemotherapy-induced premature senescence and facilitate apoptosis in human glioblastoma cells. Int J Cancer. 2010; 127:1240–1248. [PubMed: 20099278]
41. Klein S, de Fougerolles AR, Blaikie P, Khan L, Pepe A, Green CD, et al. Alpha 5 beta 1 integrin activates an NF-kappa B-dependent program of gene expression important for angiogenesis and inflammation. Mol Cell Biol. 2002; 22:5912–5922. [PubMed: 12138201]

42. Shain KH, Yarde DN, Meads MB, Huang M, Jove R, Hazlehurst LA, et al. Beta1 integrin adhesion enhances IL-6-mediated STAT3 signaling in myeloma cells: implications for microenvironment influence on tumor survival and proliferation. Cancer Res. 2009; 69:1009–1015. [PubMed: 19155309]
43. Hsu CP, Chen YL, Huang CC, Chou CC, Liu CL, Hung CH, et al. Anti-interleukin-6 receptor antibody inhibits the progression in human colon carcinoma cells. Eur J Clin Invest. 2011; 41:277–284. [PubMed: 21114487]
44. Park CC, Zhang H, Pallavicini M, Gray JW, Baehner F, Park CJ, et al. Beta1 integrin inhibitory antibody induces apoptosis of breast cancer cells, inhibits growth, and distinguishes malignant from normal phenotype in three dimensional cultures and in vivo. Cancer Res. 2006; 66:1526–1535. [PubMed: 16452209]
45. Khalili P, Arakelian A, Chen G, Plunkett ML, Beck I, Parry GC, et al. A non-RGD-based integrin binding peptide (ATN-161) blocks breast cancer growth and metastasis in vivo. Mol Cancer Ther. 2006; 5:2271–2280. [PubMed: 16985061]
46. Isaji T, Sato Y, Fukuda T, Gu J. N-glycosylation of the I-like domain of beta1 integrin is essential for beta1 integrin expression and biological function: identification of the minimal N-glycosylation requirement for alpha5beta1. J Biol Chem. 2009; 284:12207–12216. [PubMed: 19261610]
47. Bhaskar V, Fox M, Breinberg D, Wong MH, Wales PE, Rhodes S, et al. Volociximab, a chimeric integrin alpha5beta1 antibody, inhibits the growth of VX2 tumors in rabbits. Invest New Drugs. 2008; 26:7–12. [PubMed: 17786386]
48. Levkau B, Kenagy RD, Karsan A, Weitkamp B, Clowes AW, Ross R, et al. Activation of metalloproteinases and their association with integrins: an auxiliary apoptotic pathway in human endothelial cells. Cell Death Differ. 2002; 9:1360–1367. [PubMed: 12478473]
49. Mino K, Ozaki M, Nakanishi K, Haga S, Sato M, Kina M, et al. Inhibition of nuclear factor-kappaB suppresses peritoneal dissemination of gastric cancer by blocking cancer cell adhesion. Cancer Sci. 2011; 102:1052–1058. [PubMed: 21288284]
50. Kesanakurti D, Chetty C, Bhoopathi P, Lakka SS, Gorantla B, Tsung AJ, et al. Suppression of MMP-2 Attenuates TNF-alpha Induced NF-kappaB Activation and Leads to JNK Mediated Cell Death in Glioma. PLoS One. 2011; 6:e19341. [PubMed: 21573233]
51. Li R, Li G, Deng L, Liu Q, Dai J, Shen J, et al. IL-6 augments the invasiveness of U87MG human glioblastoma multiforme cells via up-regulation of MMP-2 and fascin-1. Oncol Rep. 2010; 23:1553–1559. [PubMed: 20428809]
52. Zhang X, Yin P, DI D, Luo G, Zheng L, Wei J, et al. IL-6 regulates MMP-10 expression via JAK2/STAT3 signaling pathway in a human lung adenocarcinoma cell line. Anticancer Res. 2009; 29:4497–4501. [PubMed: 20032397]
53. Ara T, DeClerck YA. Interleukin-6 in bone metastasis and cancer progression. Eur J Cancer. 2010; 46:1223–1231. [PubMed: 20335016]
54. Rojas A, Liu G, Coleman I, Nelson PS, Zhang M, Dash R. IL-6 promotes prostate tumorigenesis and progression through autocrine cross-activation of IGF-IR. Oncogene. 2011; 30:2345–2355. [PubMed: 21258401]
55. Giannini C, Sarkaria JN, Saito A, Uhm JH, Galanis E, Carlson BL, et al. Patient tumor EGFR and PDGFRA gene amplifications retained in an invasive intracranial xenograft model of glioblastoma multiforme. Neuro-oncol. 2005; 7:164–176. [PubMed: 15831234]
56. Galatioto J, Mascareno E, Siddiqui MA. CLP-1 associates with MyoD and HDAC to restore skeletal muscle cell regeneration. J Cell Sci. 2010; 123:3789–3795. [PubMed: 20940258]
57. Kesanakurti D, Sareddy GR, Babu PP, Kirti PB. Mustard NPR1, a mammalian IkappaB homologue inhibits NF-kappaB activation in human GBM cell lines. Biochem Biophys Res Commun. 2009; 390:427–433. [PubMed: 19766095]
58. Ganji PC, Nalla AK, Gupta R, Mohanam S, Gujrati M, Dinh DH, et al. siRNA-Mediated Downregulation of MMP-9 and uPAR in Combination with Radiation Induces G2/M Cell-Cycle Arrest in Medulloblastoma. Mol Cancer Res. 2011; 9:51–66. [PubMed: 21148633]

59. Badiga AV, Chetty C, Kesanakurti D, Are D, Gujrati M, Klopfenstein JD, et al. MMP-2 siRNA Inhibits Radiation-Enhanced Invasiveness in Glioma Cells. PLoS One. 2011; 6:e20614. [PubMed: 21698233]

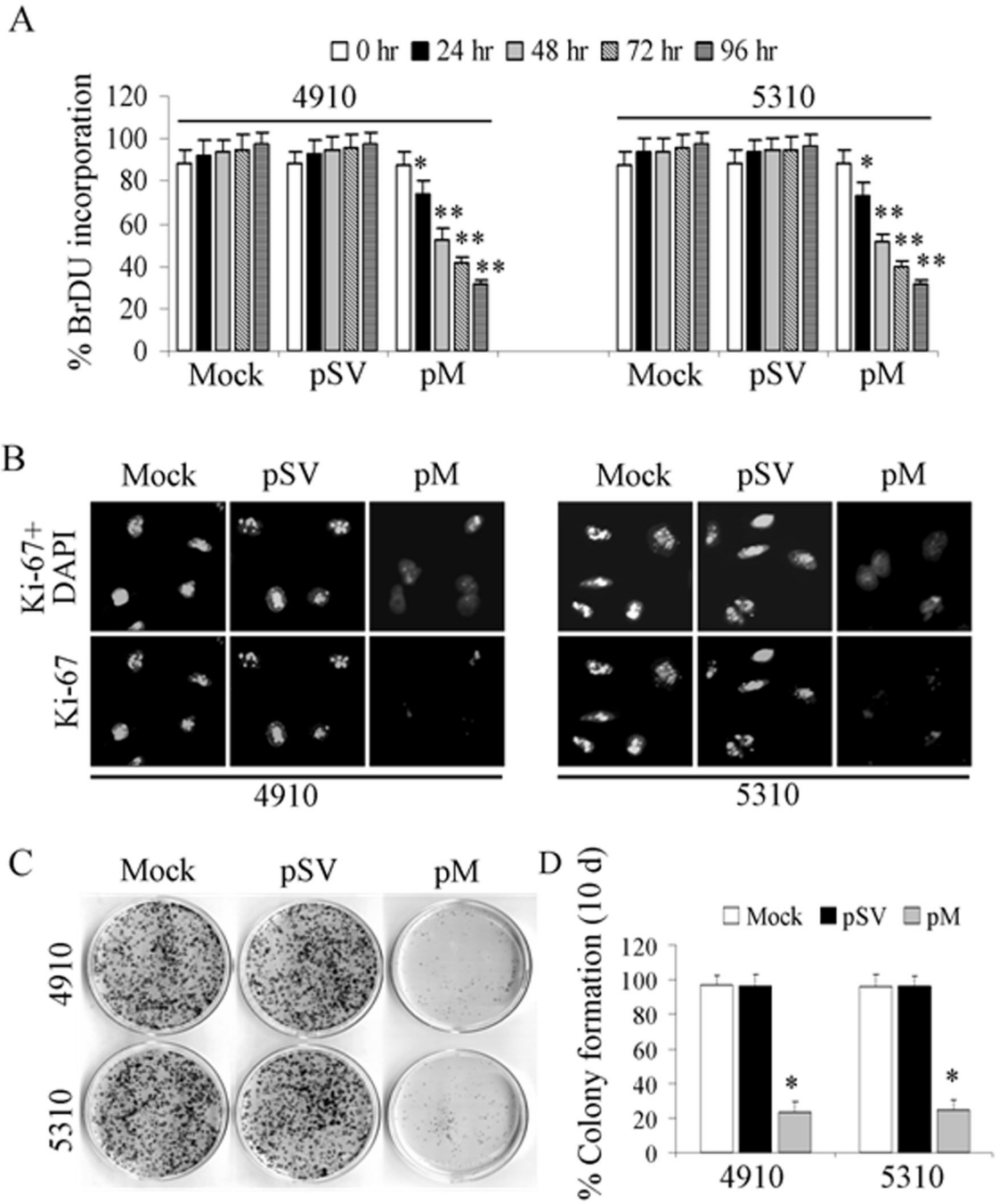

Figure 1.

Effect of MMP-2 knockdown on proliferation in 4910 and 5310 glioma xenograft cell lines. A, Proliferation rate was measured by BrDU ELISA in mock-, pSV- and pM-treated 4910 and 5310 cells at 24, 48, 72 and 92 h after transfection. Percentage of BrDU incorporation which is directly proportional to proliferation percentage was calculated and data were represented as mean ± SE of three independent replicates with significance denoted by * at $p<0.05$, and ** at $p<0.01$. B, Cells were transfected for 48 hours and subjected to Ki-67 immunostaining as described in Materials and Methods and representative confocal images

from different microscopic fields were shown. C, About 0.5×10^3 cells were seeded in 100 mm plates and were treated with mock, pSV and pM as described above. Plates were incubated for 10 days to allow colony formation, and stained with Hema-3. D, Colonies were counted under light microscope and percentage of colony formation was represented as mean±SE obtained form three independent experiments and significance was denoted by, * at $p<0.01$.

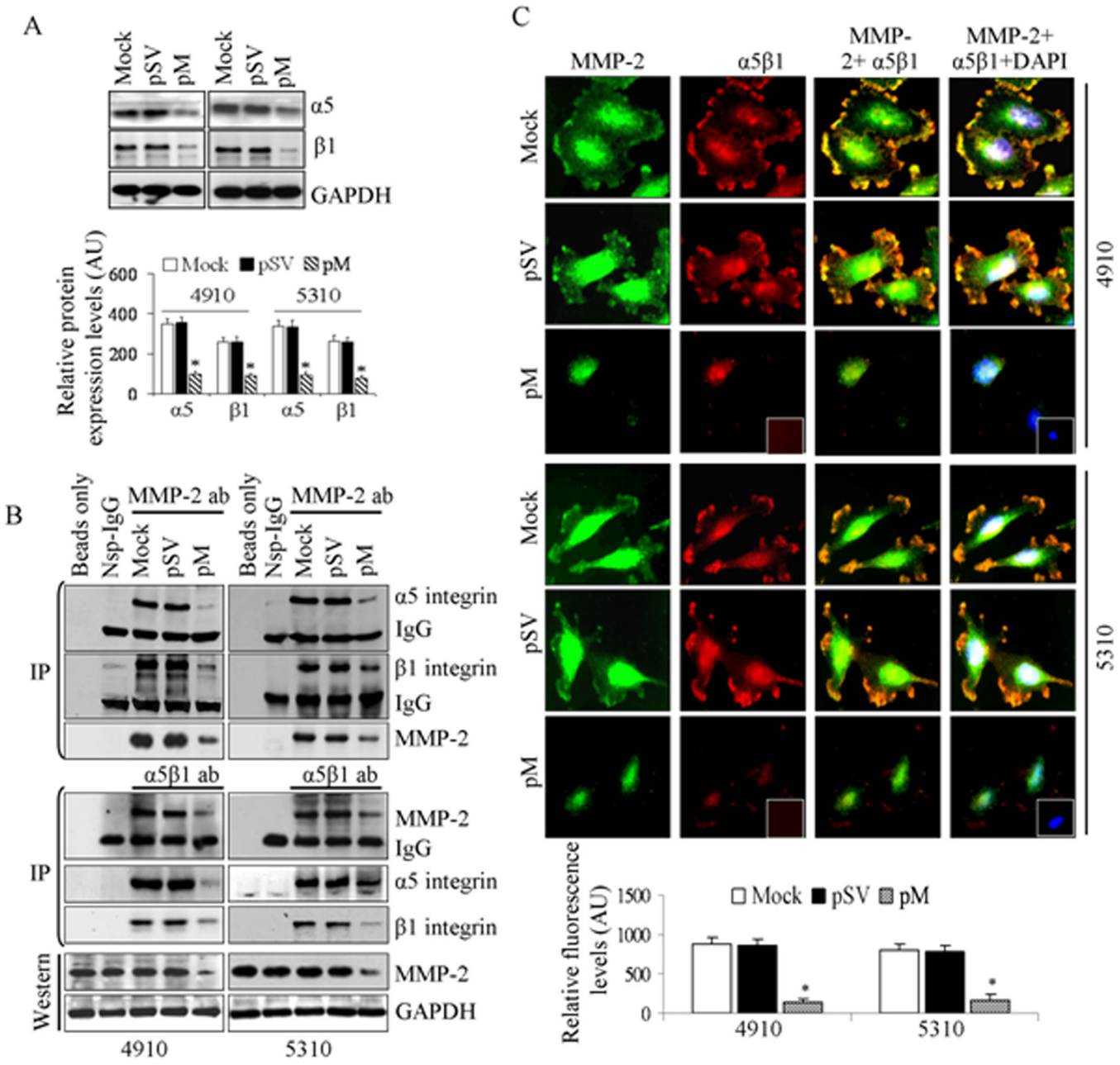

Figure 2.

Effect of MMP-2 downregulation on α5 and β1 integrin expression and MMP-2/α5β1 complex formation. A, Whole cell lysates were subjected to western blotting to check the expression levels of α5 and β1 integrins and relative expression levels were quantified using ImageJ (NIH) and plotted as mean±SE values from three replicates and statistical significance was represented by, * at $p<0.01$. B, Whole cell lysates (200 μg) were immunoprecipitated with antibodies against non-specific IgG, α5 and β1 integrin using μMACS™ protein G microbeads and MACS separation columns and immunoprecipitates were subjected to western blotting. The co-IP blots were stripped and re-probed with respective antibody used for immunoprecipitation. Input samples (whole cell lysates without

immunoprecipitation) were subjected to Western blot analysis where GAPDH probing was used to check equal loading. C, 4910 and 5310 cells were seeded in 2-well chamber slides (2×10^3 per well) and transfected for 48 h as described in Materials and Methods. Cells were fixed, permeabilized and incubated with antibodies specific for α5β1 and MMP-2 (1:100 dilution) for 2 hours at room temperature followed AlexaFluor® secondary antibodies for 1 hour, DAPI stained and mounted. Non-specific IgG staining (Nsp-IgG) served as negative control (Insets). Representative confocal microscopic pictures in randomly selected microscopic fields of three independent experimental replicates were shown. Relative florescence levels representing MMP-2/α5β1 co-localization were estimated by ImageJ 1.42 (NIH) and arbitrary units were plotted in the bar diagram as mean ± SE and significant difference among different treatment groups was denoted by * at $p<0.01$.

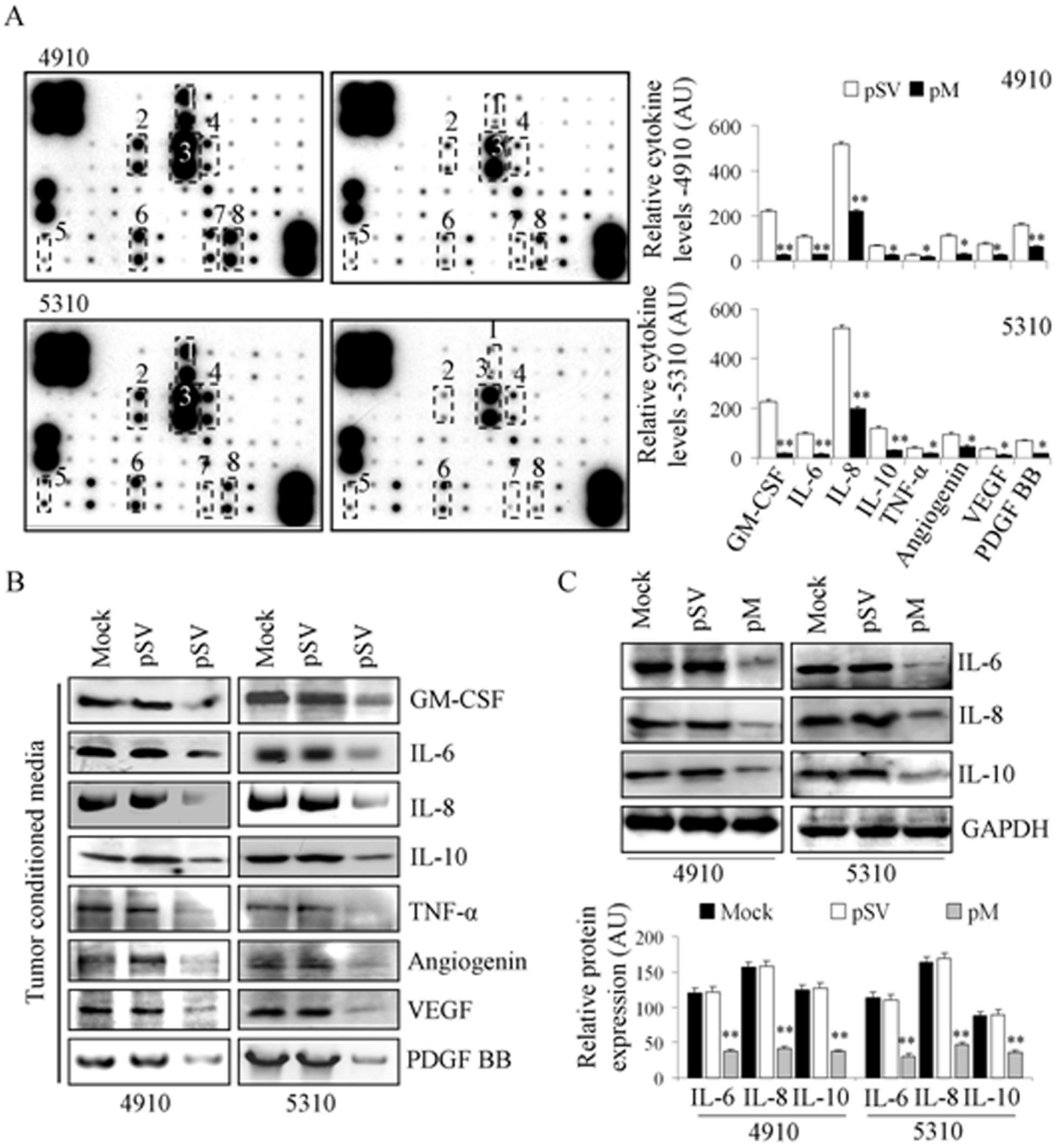

Figure 3.

Modulation of cytokine release pattern after MMP-2.siRNA (pM) treatment in 4910 and 5310 cells. A, Tumor conditioned media from pSV and pM treatments was collected as described in Materials and Methods and subjected to Western array using Ray Biotech cytokine antibody array #3 following manufacturer's instructions. The significant change in secreted among different treatments was highlighted with surrounding boxes and represent GM-CSF, IL-6, IL-8, IL-10, TNF-α, Angiogenin, VEGF and PDGF BB. The relative signal intensity was quantified using ImageJ 1.42 software (NIH) and mean±SE were plotted in the

adjacent bar diagrams where significant deviation is represented by * $p<0.05$ and ** $p<0.01$ respectively. B, Conditioned media from mock, pSV and pM treatments were subjected to Western blot analysis and the representative blots from three independent experiments were presented. C, 4910 and 5310 whole cell lysates were subjected to western blot analyses and densitometric values showing relative expression levels were plotted as mean ± SE from three experimental replicates.

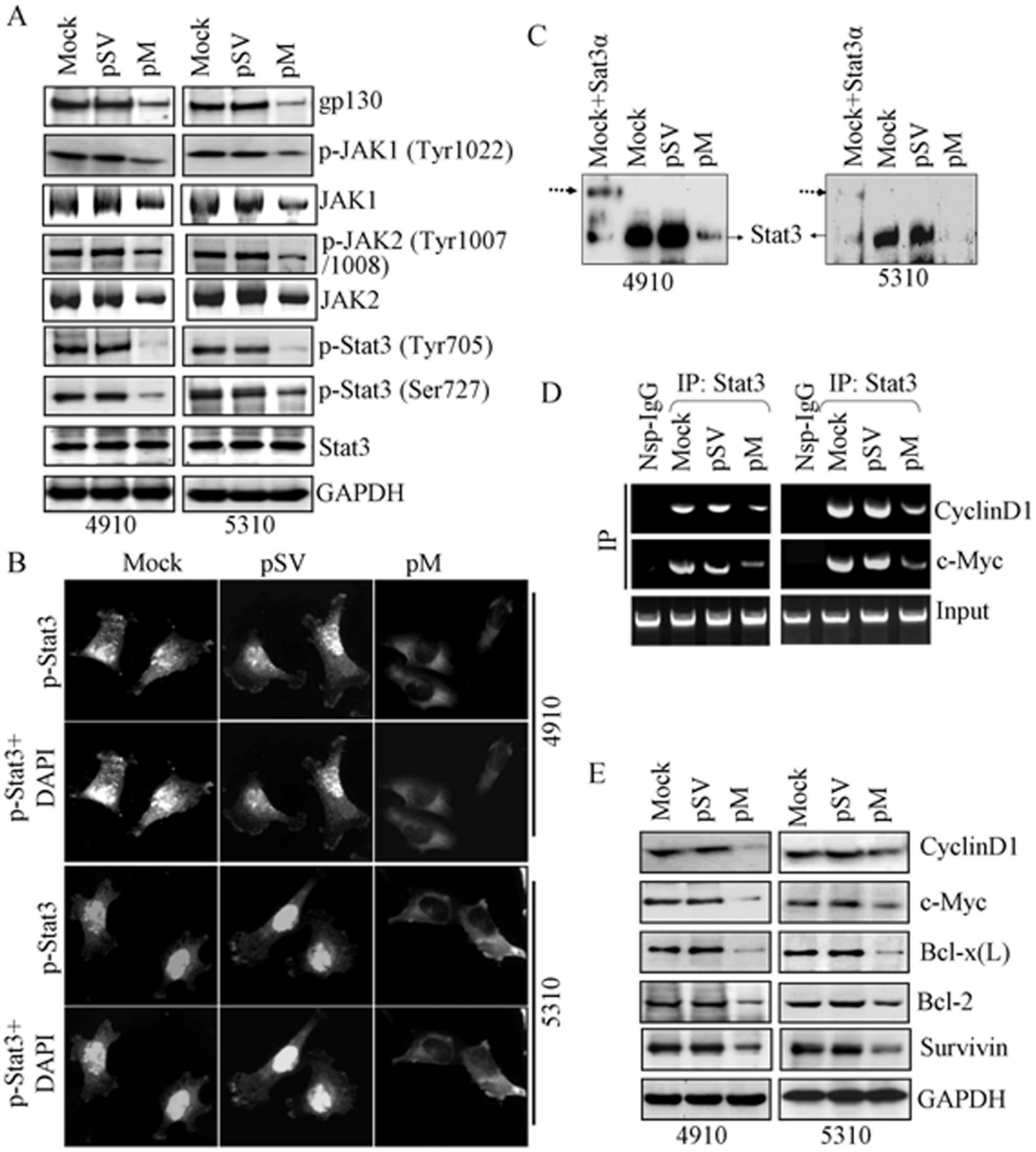

Figure 4.

MMP-2 downregulation inhibits Stat3 phosphorylation, DNA-binding activity and recruitment on to CyclinD1 and c-Myc promoters. A, At 48 h post-transfection, whole 4910 and 5310 cell lysates were subjected to Western blot analysis. Subsequently, blots were stripped and reprobed with GAPDH to confirm equal loading. B, Immunoflourescence was performed as described in Materials and Methods to analyze the expression levels of phospho-Stat3. DAPI was used for nuclear counterstaining and confocal micrographs representative of numerous randomly selected microscopic fields in at least 3 independent

experiments was shown. C, EMSA showing Stat3 DNA-binding activity. Nuclear extracts were prepared using Biovision cytoplasmic/nuclear extraction kit and subjected to EMSA using Panomics EMSA kit following manufacturer's instructions. The mock sample was pre-incubated with STAT3α antibody for 30 minutes at room temperature and then loaded for supershift and representative blots from three independent repetitions were shown. D, ChIP assay was performed in mock-, pSV- and pM-treated cells using ChIP-IT™ Express Magnetic Chromatin Immunoprecipitation kit following manufacturer's protocol (Active motif) and immunoprecipitated DNA was collected using magnetic protein G beads and the chromatin reverse cross-linked, purified and subjected to PCR to detect the Stat3 recruitment at CyclinD1 and c-Myc promoter sequences. Pre-immunoprecipitated samples were used as input controls in PCR amplification of GAPDH to monitor equal loading and IP with normal sheep IgG (Nsp-IgG) served as negative control. E, Whole 4910 and 5310 cell lysates were subjected to Western blotting and blots were re-probed with GAPDH to assure equal loading.

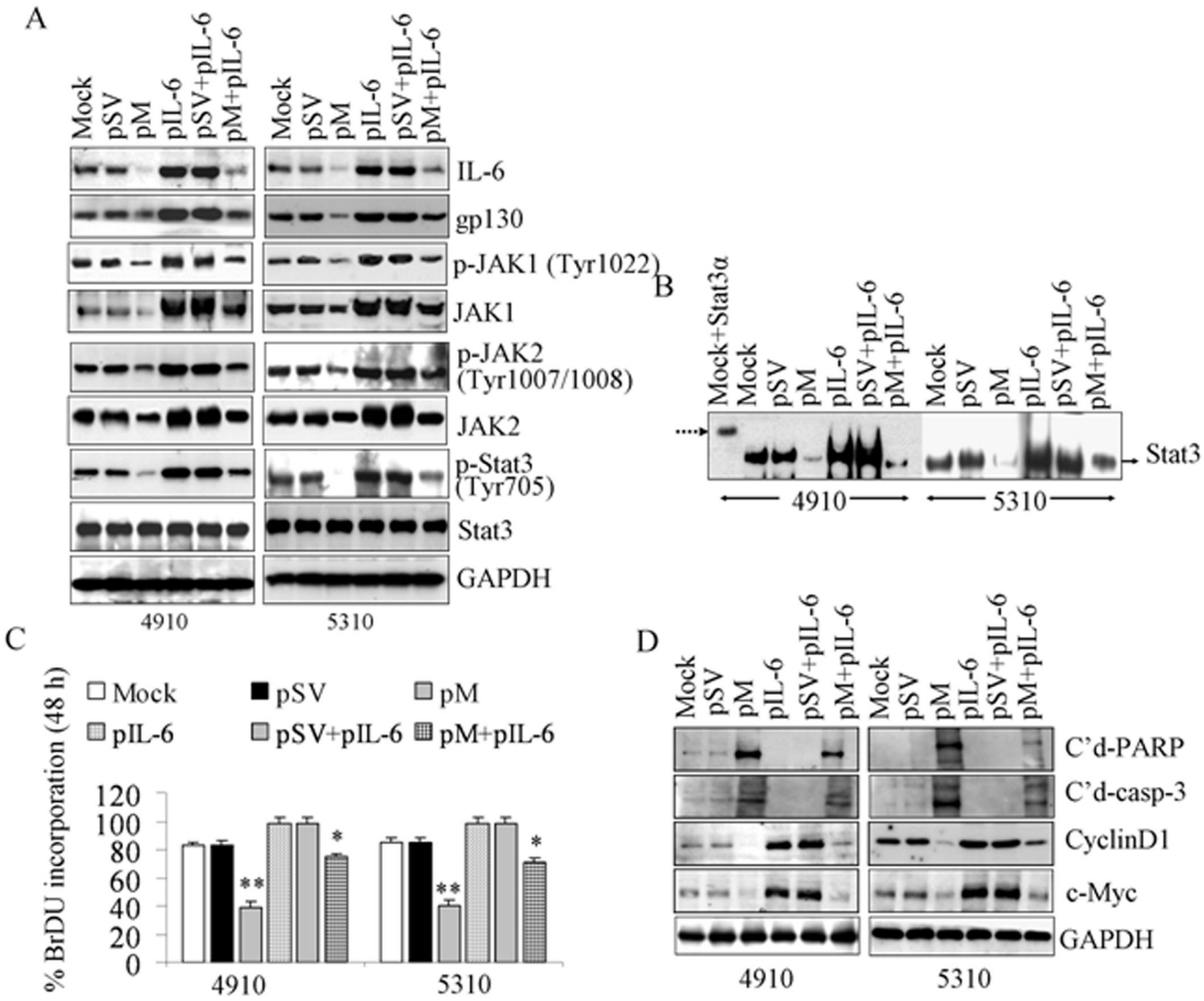

Figure 5.

Effect of IL-6 overexpression on pM-inhibited constitutive Stat3 phosphorylation, DNA-binding activity and proliferation in glioma xenograft cells. A, Western blotting was performed using 4910 and 5310 whole cell lysates at 48 hours post-transfection. GAPDH probing was used to check equal loading. B, Nuclear extracts were prepared using Biovision cytoplasmic/nuclear extraction kit and subjected to EMSA using Panomics EMSA kit as per the manufacturer's instructions. Representative blots from three independent repetitions were shown. For supershift analysis, mock sample was loaded after pre-incubation with STAT3α antibody for 30 min at room temperature. C, 4910 and 5310 cells were seeded (1×10^3 cells/well) in 96-well plates and subjected to different treatments for 48 hours as described in Materials and Methods. BrDU cell proliferation assay was performed % BrDU incorporation obtained from three individual repetitions was represented as mean±SE and significance is shown by * at $p<0.05$ and ** $p<0.01$. D, Western blotting was performed using whole cell lysates to check cleaved PARP, cleaved caspase-3, CyclinD1 and c-Myc

expression levels. Blots are representative of three experimental replicates and GAPDH probing was used to confirm equal loading.

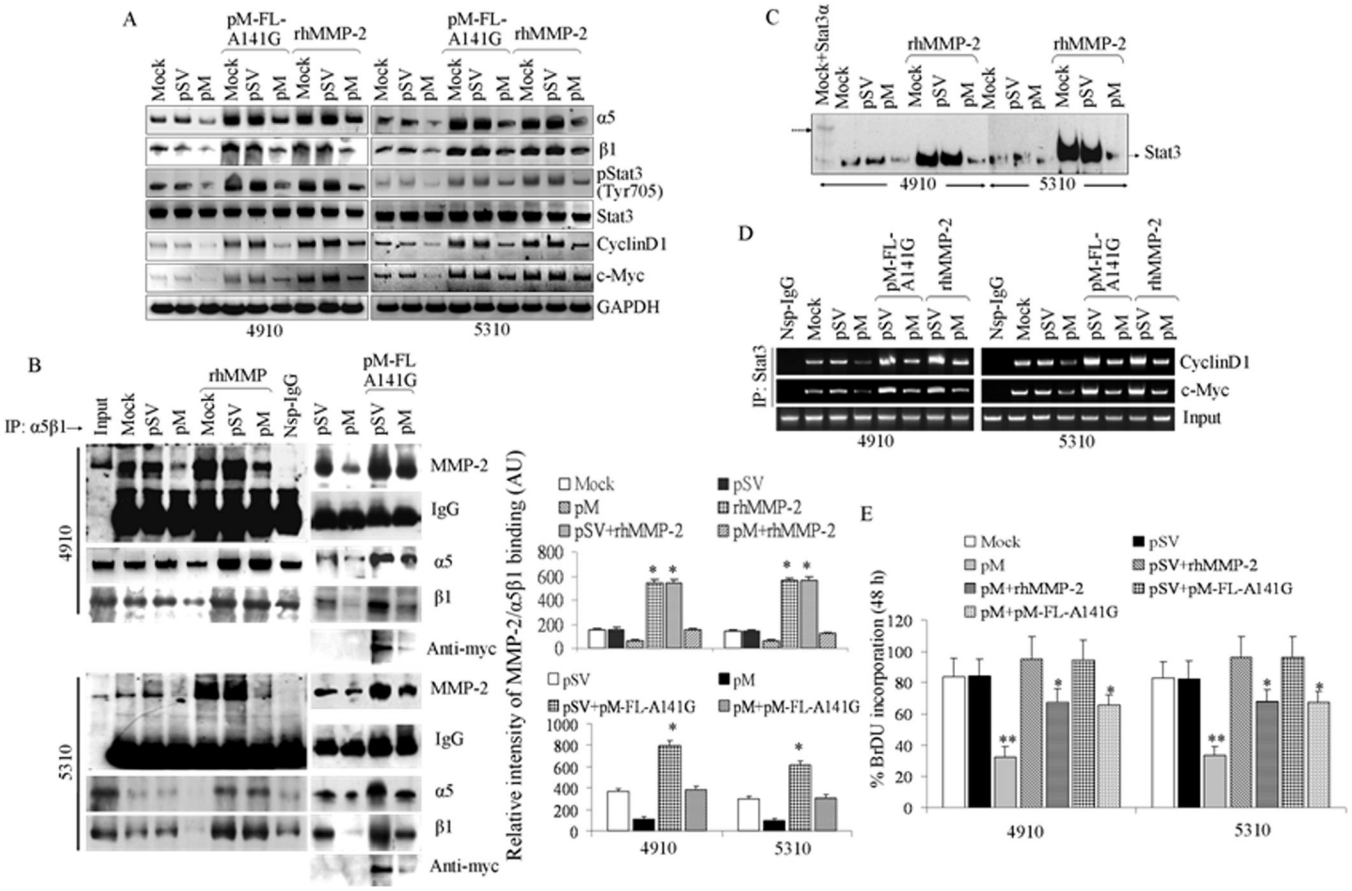

Figure 6.

Effect of siRNA-insensitive MMP-2 overexpression and rhMMP-2 supplementation on pM-inhibited IL-6/Stat3 signaling activation. A, After 48 hours of treatment with mock, pSV, pM, pM-FL-A141G, pSV+pM-FL-A141G, pM+pM-FL-A141G, rhMMP-2, pSV +rhMMP-2, and pM+rhMMP-2 as described in Materials and Methods, whole cell lysates were subjected to Western blotting. Blots were representative of at least three independent repetitions and GAPDH probing confirmed equal loading. B, Effect of MMP-2 overexpression by siRNA-insensitive pM-FL-A141G treatment or rhMMP-2 supplementation on pM-inhibited MMP-2/α5β1 integrin binding. Whole cell lysates were (200 μg each) were immunoprecipitated with anti-α5β1 integrin antibody (10 μL each sample) using μMACS™ protein G microbeads and MACS separation columns and immunoprecipitates were subjected to Western blotting. The mock sample immunoprecipitated with non-specific IgG was loaded as the negative control. Input shows whole cell lysate (50 μg) of mock sample served as the positive control. Blots were probed with anti-MMP-2 antibody and representative blots from three independent repetitions were shown. Adjacent bar diagram shows the densitometric analyses of the relative band intensity represented as mean±SE values obtained from three repetitions. The significant differences among various treatment groups were indicated by *at $p<0.05$. IP blots were stripped and subsequently re-probed with anti-α5, anti-β1 and anti-Myc antibodies. C, EMSA was performed using Panomics EMSA kit following the manufacturer's instructions as described in Materials and Methods. The mock sample was pre-incubated with Stat3α antibody for 30

minutes at room temperature and loaded for supershift. Representative blots from three experimental replicates were shown. D, ChIP assay was performed using ChIP-IT™ Express Magnetic Chromatin Immunoprecipitation kit following manufacturer's protocol (Active motif). In short, cells were fixed in 37% formaldehyde and chromatin was sheared by sonication and immunoprecipitated using anti-Stat3 antibody and normal sheep IgG (Nsp-IgG) antibodies by incubation at 4°C for 2–4 hours on a rotor. The immunoprecipitates was collected by using magnetic protein G beads (Millipore) and the chromatin was reverse cross-linked, purified and subjected to PCR to detect the Stat3 recruitment at CyclinD1 and c-Myc promoter sequences. Pre-immunoprecipitated samples were used as input controls for PCR amplification of GAPDH and normal sheep IgG (Nsp-IgG) incubation was used for the negative control. E, BrDU assay was performed following manufacturer's instructions to obtain mean±SE values of BrDU incorporation percentage from three repetitions and significance was represented by * at $p<0.05$ and ** $p<0.01$.

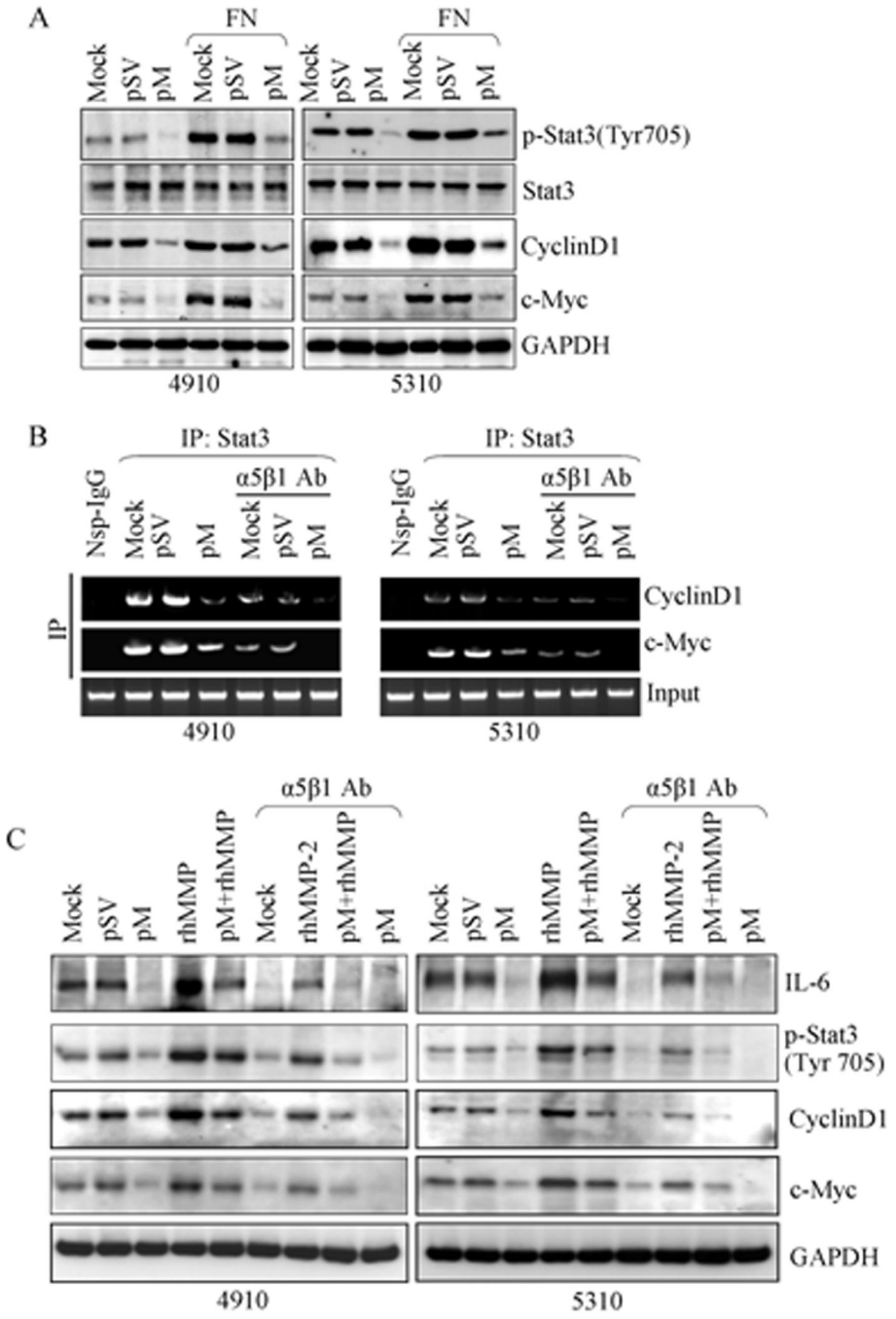

Figure 7.

Abrogation of IL-6/Stat3 activation by α5β1 integrin function blocking glioma xenograft cells. A, Effect of Fibronectin adhesion induced α5β1 signaling activation on pM-inhibited Stat3 activation. The 4910 and 5310 cells were transfected with mock, pSV and pM for 24 hours as described in Materials and Methods. Cells were detached from culture plates by trypsinization and re-plated on FN-coated plates and cultured for another 24 hours. Whole cell lysates were subjected western blotting and representative blots showing expression levels of phospho-Stat3, CyclinD1 and c-Myc were obtained from three individual

repetitions. B, ChIP assay was performed using ChIP-IT™ Express Magnetic Chromatin Immunoprecipitation kit following manufacturer's protocol (Active motif) and immunoprecipitated DNA reverse cross-linked, purified and subjected to PCR to detect the Stat3 recruitment at CyclinD1 and c-Myc promoter sequences where pre-immunoprecipitated input samples were used for GAPDH PCR amplification and normal sheep IgG (Nsp-IgG) immunoprecipitates was loaded as negative control. C, Cells were treated with mock, pSV, pM, rhMMP-2 and α5β1 blocking antibody for 48 hours as described in Materials and Methods and whole cell lysates were subjected to western blotting to determine the expression levels of IL-6, phospho-Stat3, CyclinD1 and c-Myc. Blots were stripped and re-probed with GAPDH to confirm equal loading.

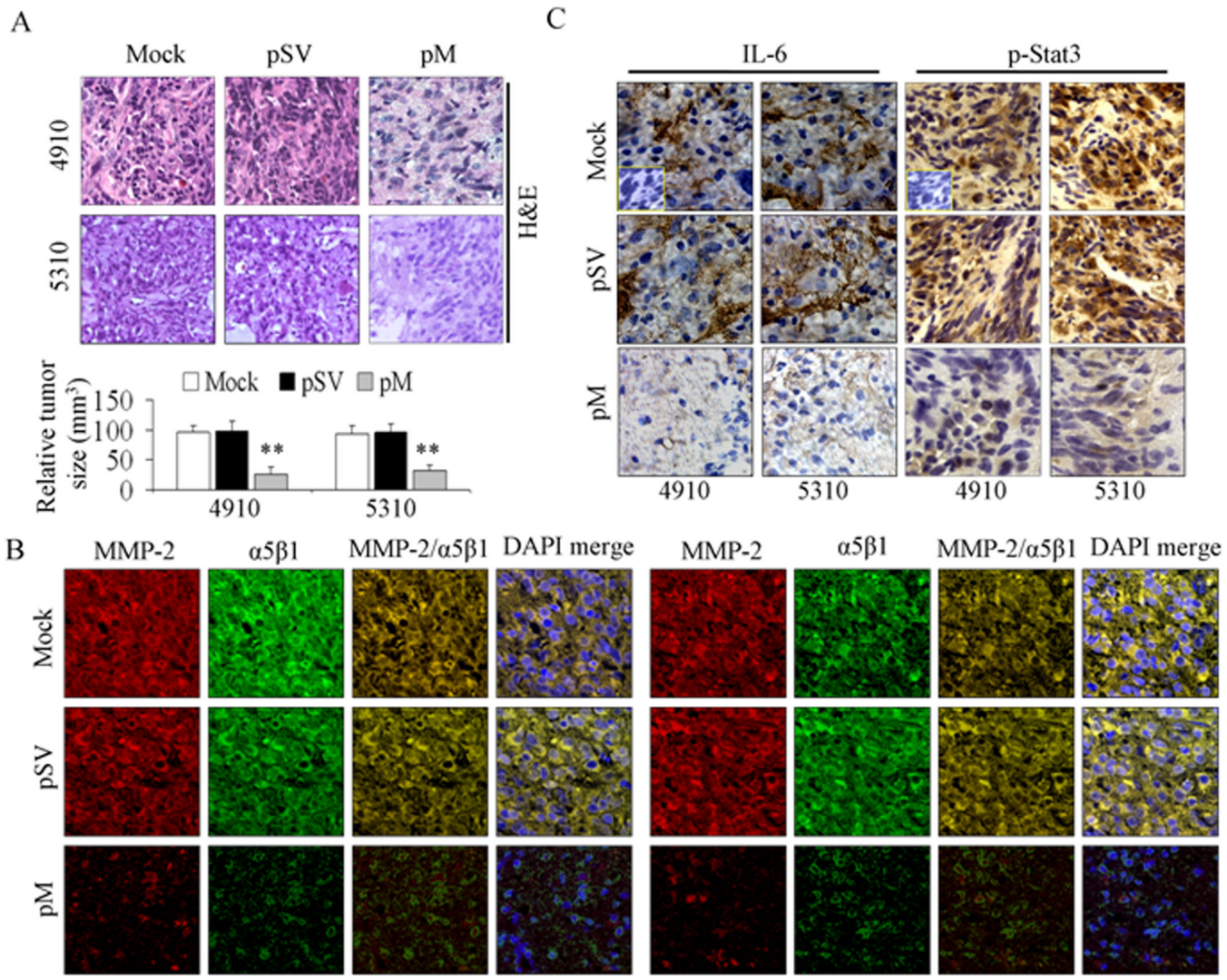

Figure 8.

Effect of MMP-2 knockdown on *in vivo* tumor growth. Tumor growth was established by intracranial injection of 4910 and 5310 cells into athymic nude mice (nu/nu) and pSV and pM plasmids were injected into the tumors as described in Materials and Methods while sterile 1×PBS injection served as mock treatment. A, Hematoxylin and eosin staining of brain sections displaying the neoplastic growth of tumors. The relative brain tumor size was plotted as mean±SE obtained from three sets of treatment groups (n=10) and the significance is represented by ** at $p<0.01$. B, Immunoflorescence showing co-localization of MMP-2 and α5β1 integrin in tumor sections. The deparaffinized mock, pSV-, and pM-treated tumor sections were passed through graded ethanol series, blocked with 1% BSA, and incubated with anti-MMP-2 and anti-α5β1 integrin antibodies (1:100) overnight at 4°C. Sections were washed and incubated with specific Alexa Fluor® antibodies and counterstained with DAPI and observed for cellular MMP-2 and α5β1 expression. Depicted pictures are representative of 20 different sections from each set of treatments (n=10). C, Immunocytochemical DAB staining showing IL-6, phospho-Stat3 (Tyr 705) expression in

tumor sections. Hematoxylin was used for nuclear counter staining. Negative control staining was performed by incubation with non-specific IgG (Insets).

Table 1
Gene expression changes in pSV- and pMMP-2.siRNA-tretaed 4910 and 5310 cells

Total RNA was isolated from pSV- and pM-treated 4910 and 5310 cells using TRIzol (Invitrogen) and cDNA was synthesized from 1μg RNA. The cDNA was analyzed with human JAK/STAT signaling pathway RT^2 Profiler™ PCR array system using SYBR Green/fluorescein qPCR master mix (SA Biosciences). The resulting gene expression changes in the form of Ct values were analyzed and converted in to fold changes and compared with the web-based software package for PCR array system. The mean fold change in expression levels in pM- and pSV-treatments was obtained from three independent experiments.

Gene name	NCBI REFSEQ	Description	pMMP-2.si/pScrambled vector	
			4910 cells	5310 cells
			~fold	~fold
JAK1	NP_002218	Janus kinase 1	0.22	0.28
JAK2	NP_004963	Janus kinase 2	0.31	0.41
EGFR	NP_005219	Epidermal growth factor receptor	0.12	0.19
Stat2	NP_005410	Signal transducer and activator of transcription 2	0.33	0.31
Stat5	NP_036580	Signal transducer and activator of transcription 5	0.26	0.23
CSF1R	NP_005202	Colony stimulating factor 1 receptor	0.13	0.18
CSF2RB	NP_000386	Colony-stimulating factor-2 receptor, beta, low-affinity	0.23	0.24
EPOR	NP_000112	Erythropoietin receptor	0.21	0.23
IFNAR1	NP_000620	Interferon (alpha, beta and omega) receptor 1	0.16	0.25
IL10RA	NP_001549	Interleukin 10 receptor, alpha	0.20	0.22
CRK	NP_005197	Proto-oncogene c-Crk	0.21	0.18
IL2RG	NP_000197	Interleukin 2 receptor, gamma	0.26	0.26
IL4R	NP_000409	Interleukin 4 receptor	0.16	0.18
IL6ST	NP_001177910	IL-6 receptor subunit beta	0.10	0.09
INSR	NP_000199	Insulin receptor	0.31	0.24
MPL	NP_005364	Myeloproliferative leukemia virus oncogene	0.31	0.27
PDGFRA	NP_006197	Platelet-derived growth factor receptor, α polypeptide	0.40	0.35
SH2B1	NP_001139267	SH2B adaptor protein 1	0.36	0.25
SRC	NP_005408	Proto-oncogene c-Src	0.30	0.21
F2	NP_000497	Coagulation factor II (thrombin)	0.31	0.34
F2R	NP_001983	Coagulation factor II (thrombin) receptor	0.33	0.26
IL20	NP_061194	Interleukin20	0.22	0.27
HMGA	NP_003474	High mobility group AT-hook 2	0.27	0.26
JUNB	NP_002220	Activator protein 1	0.33	0.41
SP1	NP_003100	Sp1 transcription factor	0.40	0.44
USF1	NP_009053	Upstream transcription factor 1	0.30	0.32
SMAD1	NP_001003688	SMAD family member 1	0.44	0.33
NFKB1	NP_001158884	Nuclear factor of kappa gene enhancer in B-cells 1	0.24	0.17
GATA3	NP_001002295	GATA binding protein 3	0.26	0.28
ISGF3G	NP_006075	Interferon-stimulated gene factor 3 gamma	0.35	0.30
MYC	NP_002458	Proto-oncogene c-Myc	0.07	0.09

Gene name	NCBI REFSEQ	Description	pMMP-2.si/pScrambled vector	
			4910 cells	5310 cells
CEBPB	NP_005185	CCAAT/enhancer binding protein (C/EBP), beta	0.17	0.14
CXCL9	NP_002407	Chemokine (C-X-C motif) ligand 9	0.18	0.19
IRF1	NP_002189	Interferon regulatory factor 1	0.22	0.27
FCGR1A	NP_001992	Fc fragment of IgG, high affinity Ia, receptor (CD64)	0.23	0.28
NOS2A	NP_000616	Nitric oxide synthase 2, inducible	0.23	0.22
A2M	NP_000005	Alpha-2-macroglobulin	0.25	0.33
BCL2L1	NP_001182	BCL2-like 1	0.33	0.28
MMP3	NP_002413	Mtrix metallopeptidase 3 (stromelysin 1)	0.21	0.20
CCND1	NP_444284	Cyclin D1	0.12	0.13
IL2RA	NP_000408	Interleukin 2 receptor, alpha	0.15	0.12
OSM	NP_065391	Oncostatin M	0.34	0.33
SMAD3	NP_001138574	SMAD family member 3	5.4	4.7
PIAS1	NP_057250	protein inhibitor of activated STAT, 1	7.6	6.3
SOCS1	NP_003736	Suppressor of cytokine signaling 1	11.1	10.6
FAS	NP_000034	Fas (TNF receptor superfamily, member 6)	8.2	6.5
JUN	NP_002219	Proto-oncogene c-Jun	3.1	4.5
PPP2R1A	NP_055040	Potein phosphatase 2, regulatory subunit A, alpha	7.6	5.4
PRLR	NP_000940	Polactin receptor	3.4	3.3
CDKN1A	NP_000380	Cyclin-dependent kinase inhibitor 1A (p21, Cip1)	8.7	7.0